CHAPTER 3 RESULTS AND DISCUSSIONS

3.0 Synthesis of Silk Fibroin / N, N' methylene diacrylamide Biofilms

For the film-casting fabrication we used N, N' methylene diacrylamide crosslinker and UV-irradiation, which is considered to be more versatile, practical and non-toxic process because limited amount of chemicals can be use and less parameters affects the quality of the final cast biofilms. The synthesis reactions were carried out at various wavelengths (254 nm and 365 nm) and crosslinker ($C_7H_{10}N_2O_2$) concentrations as shown in Table 3.1. In the following, the formation, swelling, biodegradability and morphologic properties of silk fibroin biofilms are discussed as depending on the synthesis parameters. Then, the blood clotting and platelet adhesion properties analyzed, discussed The aqueous silk fibroin concentrations obtained were 3% w/v, 4% w/v, 5% w/v, 6% w/v SF/ electrolyte solution but those ratios were not exact concentrations because an amount of distilled water diffused into the membrane during the dialysis process. After the dialysis process, concentrations of solution were decreased about half of the original concentration, 3%, 4%, 5%, and 6%, before dialysis process became 1.5%, 2%, 2.5%, 3%, after dialysis. Practical technique used to calculate the real concentrations of protein; from 6% aqueous silk fibroin solution a biofilm was prepared by using 1ml of the silk solution the amount of protein was 0.0297 g/ml, which it is 2.97 % w/v.

. Table 3.1: Silk fibroin biofilms samples.

Samples	$C_7H_{10}N_2O_2$ Crosslinker volume	SF Volume & Concentration	Ultraviolet (UV) Wavelength
SS1	0μl		
SS2	25μl		
SS3	50μl	2 ml Silk Fibroin Solution	Short wave (254nm)
SS4	125μl	3%	
SS5	150μl		
SL1	0 μl		
SL2	25μl		
SL3	50μl	2 ml Silk Fibroin Solution	Long wave (365nm)
SL4	125μl	3%	
SL5	150μl		

The prepared SF / N, N' methylene diacrylamide biofilms are stable in toluene and acetone, and after treatment with methanol, their resistance to water treatment increases dramatically resulting in no obvious signs of dissolution observed after water treatment.

3.1 Swelling Test

The swelling test results for samples which were prepared in different reaction conditions with ABS or PBS solutions were discussed in this section. The human physiological fluids pH range is change in between pH = 1 to 9, and human gastric fluid has approximately 1.2 pH value, gastrointestinal juice pH value is approximately 7.4, respectively. To estimate swelling behavior of biofilms *in vitro* conditions, SF/N, N' methyelene diacrylamide biofilms were soaked in 40 ml of ABS and PBS solutions separately at 37°C and their behavior were evaluated. The swelling ratios of biofilms were different depending on the amount of crosslinker and wave length. In contrast, after a period of time samples were reached the equilibrium swelling ratio no matter which buffer solution was used. The swelling data were shown in the Tables 3.2, 3.5, 3.8, 3.11.


Figure 3.1: Swelling test for SF biofilms with ABS and PBS.

3.1.1 Swelling test for SF biofilms UV-Short wave with ABS

Table 3.2: Swelling test values of SF biofilms UV-Short wave with ABS (pH = 1.2)

| Time (Hours)	SS1 weight	SS2 weight	SS3 weight	SS4 weight	SS5 weight
0	12.5	12.3	12.1	11.9	12.2
0.25	27.7	24.8	22.5	20.32	18.97
0. 5	28.3	25.7	23.98	21.11	20
0.75	33.2	27.73	24.32	22	20.89
1	36.1	29.99	25.61	23.41	21.34
1.5	38	33.76	27.41	24.98	22.10
2	40.12	35.21	28	26.12	22.99
24	41.8	36	29.53	27.63	23.5
48	42.2	37.2	31.43	28.79	24.38
96	43.9	39.11	32.1	29	26
120	44.2	40.31	32.4	29.3	26.43
144	44.8	40.85	32.6	29.7	26.79
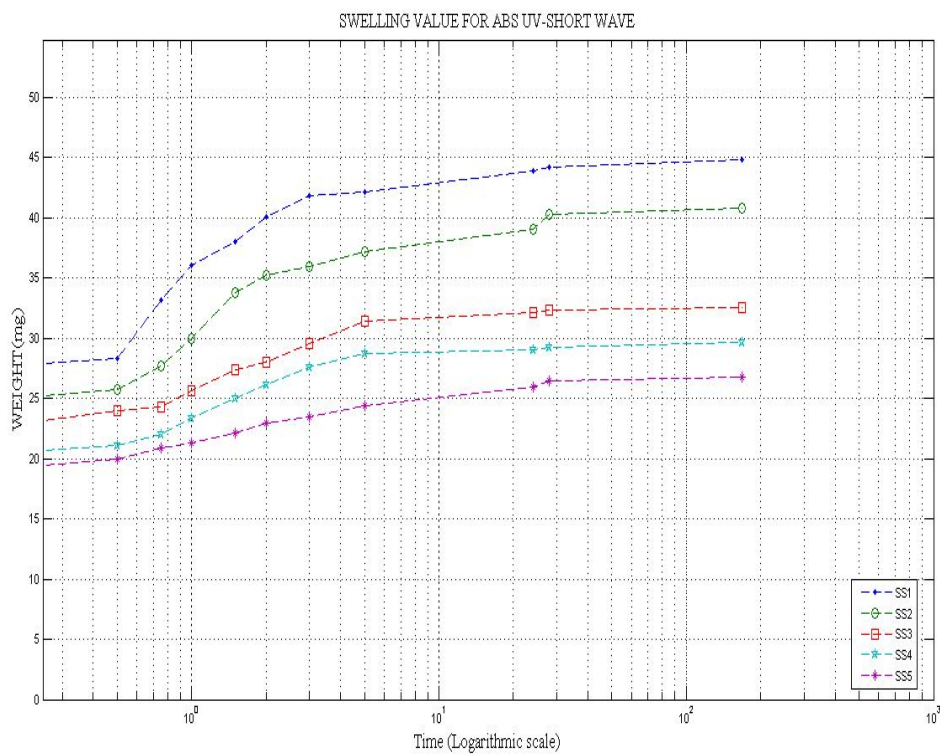
Figure 3.2: Swelling test values for SF biofilms UV-Short wave with ABS.

36

The swelling test results showed that the samples without or with little amount of crosslinker swelled more than the samples with greater amount of crosslinker as shown in Table 3.2, Fig.3.2. As the amount of N, N' methylene diacrylamide increases the crosslinking ratio also increases and the swelling ratio decreases. They are inversely proportional to each other.

Table 3.3: Swelling standard deviation for SF biofilms UV-Short wave with ABS.

| Samples	Total Numbers	Mean	Standard deviation	Variance(Standard deviation)	Population Standard deviation	Variance(Population Standard deviation)
SS1	12	36.06833	9.47901	89.85167	9.07546	82.36403
SS2	12	31.91333	8.29115	68.74321	7.93817	63.01461
SS3	12	26.83167	5.83001	33.98898	5.58181	31.15656
SS4	12	24.52167	5.19215	26.95843	4.97111	24.7119
SS5	12	22.1325	4.02437	16.19558	3.85304	14.84595
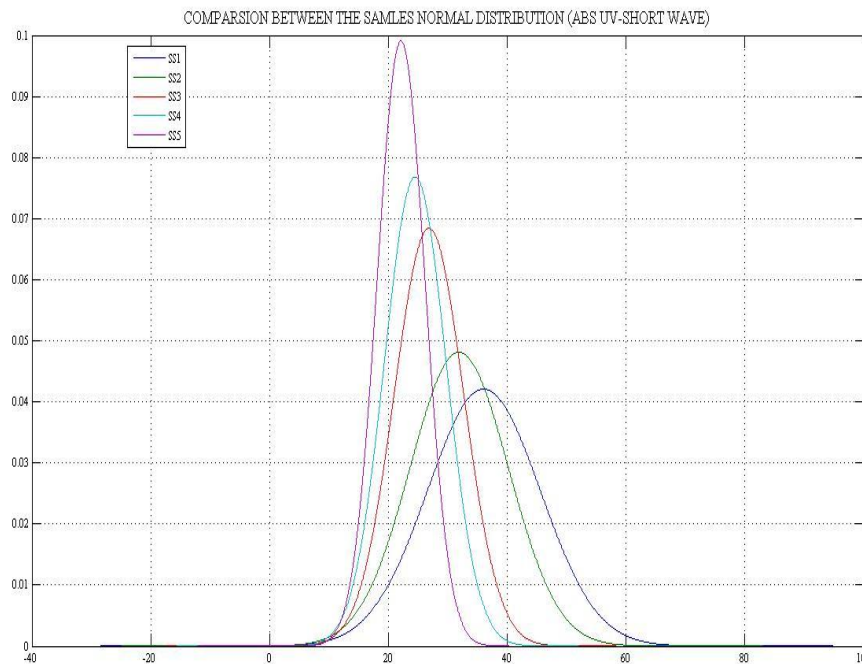
Figure 3.3: Normal distribution for SF Biofilms UV-Short wave with ABS.

Standard deviation used to show how much variation or dispersion exists from the average (mean), or expected value. A low standard deviation indicates that the data points tend to be very close to the mean and high standard deviation indicates that the data points are spread out over a large range of values and the standard deviation calculated by equations number 4, 5, 6. According to the results of the standard deviation of silk fibroin biofilms UV-Short wave with ABS swelling as showed in Table 3.3 and Figure 3.3, the sample SS5 has the lowest standard deviation value and mean. SS5 was prepared with 150 μl of $C_7H_{10}N_2O_2$ cross linker. The sample SS1 which was prepared by without crosslinker has the highest standard deviation value and mean.

$$SD = \sqrt{\frac{\sum(X-M)^2}{n-1}} \tag{4}$$

$$PSD = \sqrt{\frac{\sum(X-M)^2}{n}} \tag{5}$$

$$Variance = SD^2 \tag{6}$$

Where:

SD = Standard Deviation

PSD= Population Standard Deviation

$\sum$ = sum of

X= Individual score

M= Mean of the scores

N = Sample size (Number of scores)

The statistical results indicated that the stability of biofilms improved as the crosslinker amount increases during the synthesis. More crosslinked biofilms are more stable and swell less ABS. However, they reached at the equilibrium swelling ratio approximately at the same value.

Table 3.4: Swelling ratios for SF biofilms UV-Short wave with ABS.

| Time(Hours)	SS1 weight	SS2 weight	SS3 weight	SS4 weight	SS5 weight
0	0	0	0	0	0
0.25	121.6	101.62	85.95	70.75	55.49
0. 5	126.4	108.94	89.18	77.39	63.93
0.75	165.6	125.44	100.99	84.87	71.22
1	188.8	143.82	111.65	96.72	74.91
1.5	204	174.47	126.52	109.91	81.14
2	220.96	186.26	131.40	119.49	88.44
24	234.4	192.68	144.04	132.18	92.62
48	237.6	202.43	159.75	141.93	99.83
96	251.2	217.96	165.28	143.69	113.11
120	253.6	227.72	167.76	146.21	116.63
144	258.4	232.11	169.42	149.57	119.59
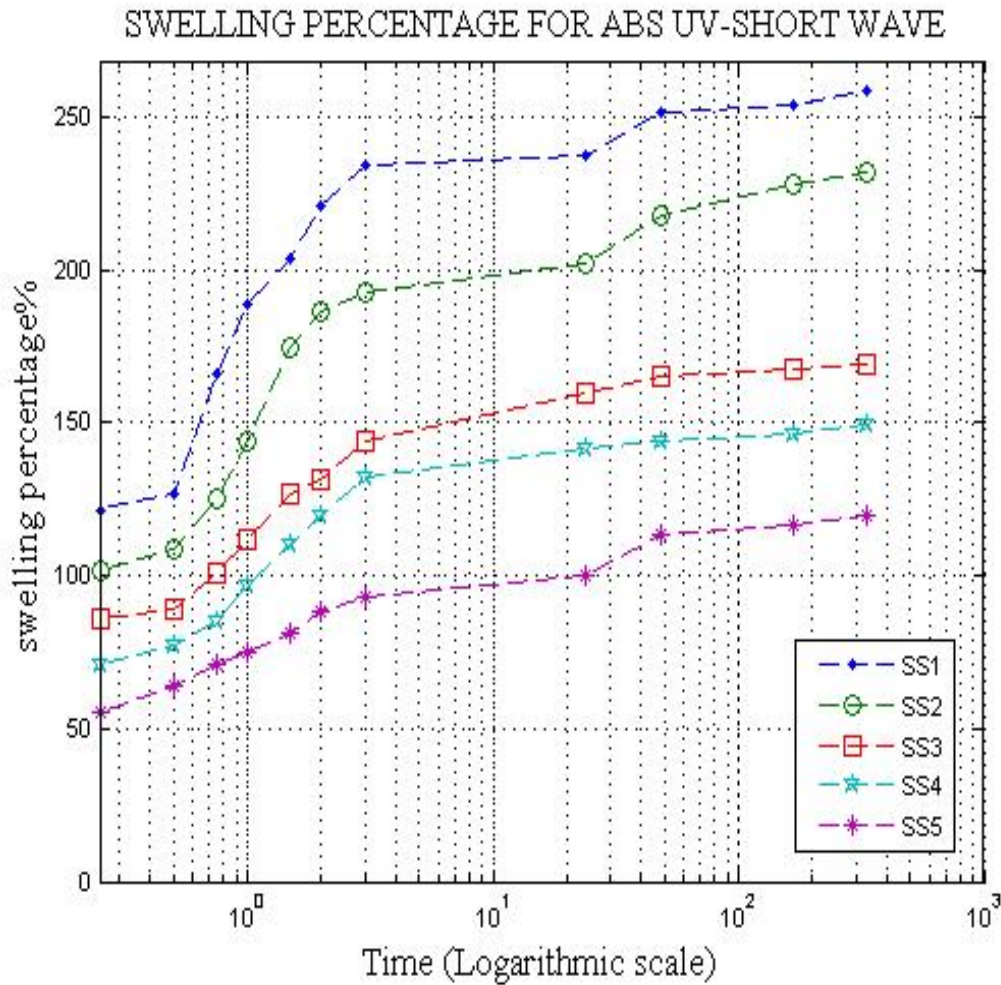
Figure 3.4: Swelling ratios of SF biofilms UV-Short wave with ABS.

The swelling ratios were determined by using equation (1) and shown on Table 3.4 and Fig 3.4. For the acid buffer solution (pH = 1.2) sample which was pure silk fibroin biofilm increase in terms of swelling until it reached to its equilibrium swelling ratio value. However, it had the highest swelling ratio compared to the low crosslinked silk fibroin biofilm with the highly crosslinked silk fibroin biofilms. These indicate that as the crosslinker content increases in the biofilm the equilibrium swelling ratio decreases.

3.1.2 Swelling Test for Biofilms UV-Long wave (365nm) with ABS

The same swelling test procedure was applied to the samples which were prepared by UV long wavelength (365 nm). The biofilms prepared at short wavelength had an effect on the swelling ratios which was inversely proportional to the crosslinker. By comparing with the biofilms prepared by long UV wavelengths, they had a slower swelling and their final swelling ratio surpasses all the other biofilms prepared at long wavelength. This was related

with the crosslink ratio of the UV-photo polymerization reaction. As the crosslink ratio increases biofilms becomes messier and pore sizes were decreased. As the results were shown on Table 3.5 and Fig 5.3

Table 3.5: Swelling test values of SF biofilms UV-Long wave with ABS.

Time(Hours)	SL1(w)	SL2(w)	SL3(w)	SL4(w)	SL5(w)
0	14.3	14.6	13.8	14.1	13.9
0.25	32.11	27.7	24.2	22	19.4
0. 5	33.4	29.2	25.1	22.9	20.7
0.75	34.3	30.8	25.9	23.6	22.6
1	35.9	32	26.4	24.9	23.4
1.5	37.3	33.9	27.1	25.1	24
2	39.1	34.7	29.5	26.9	25.3
24	40.8	35.2	30.4	27.5	26
48	45.9	39.7	31.9	28.3	26.9
96	46.3	41.6	33.3	29.9	27.5
120	46.6	42	33.9	30.7	28
144	46.9	42.4	34.2	31	28.5
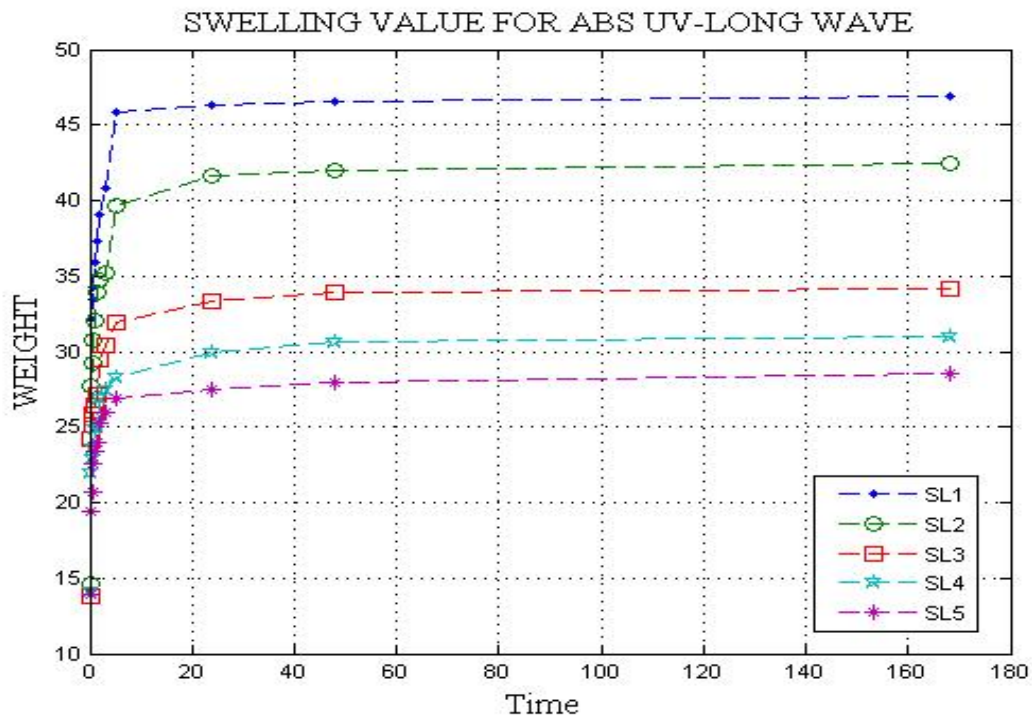
Figure 3.5: Swelling values of SF biofilms UV-Long wave with ABS.

41

Table 3.6: Swelling standard deviation for SF biofilms UV-Long wave with ABS.

Samples	Total Numbers	Mean	Standard deviation	Variance(Standard deviation)	Population Standard deviation	Variance(Population Standard deviation)
SL1	12	37.7425	9.18921	84.44149	8.79799	77.4047
SL2	12	33.65	7.85441	61.69182	7.52003	56.55083
SL3	12	27.9583	5.7078	32.57902	5.46481	29.8641
SL4	12	25.575	4.70476	22.13477	4.50447	20.29021
SL5	12	23.85	4.25024	18.06455	4.0693	16.55917
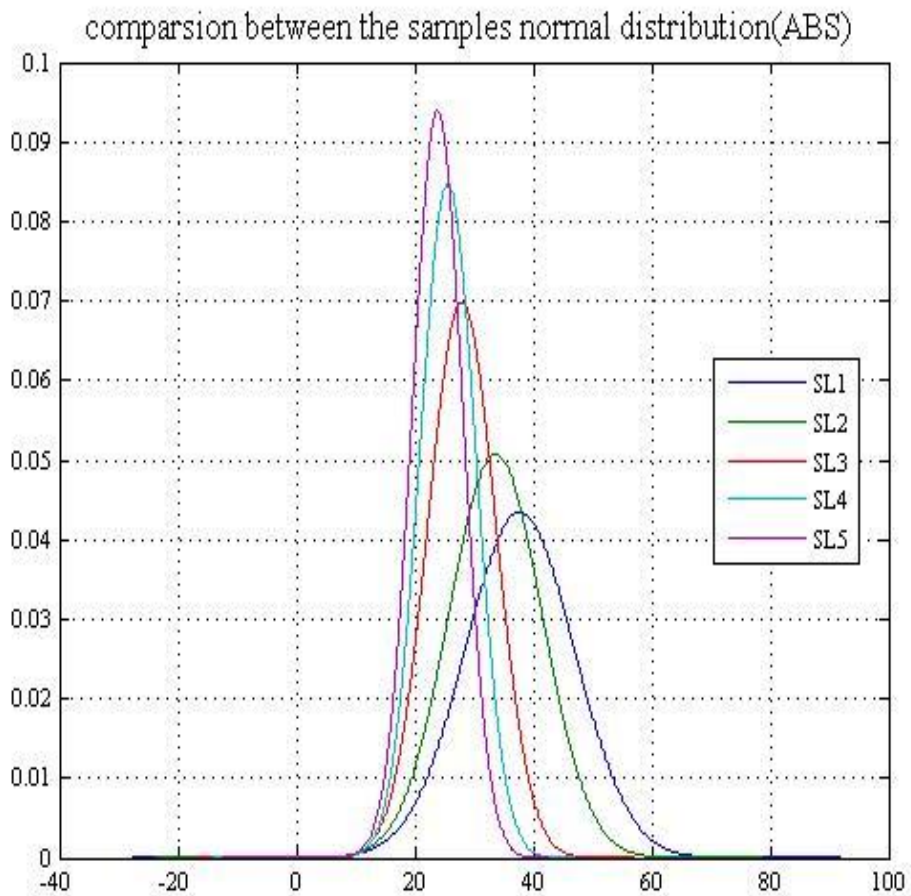
Figure 3.6: Normal distribution Biofilms UV-Long waves with ABS.

Table 3.7: Swelling test ratios of the SF biofilms UV-Long with ABS.

| Time(Hours)	SL1(w)	SL2(w)	SL3(w)	SL4(w)	SL5(w)
0	0	0	0	0	0
0.25	124.54	89.72	75.36	56.02	39.56
0. 5	133.56	100	81.88	62.41	48.92
0.75	139.86	110.95	87.68	67.37	62.58
1	151.04	119.17	91.30	76.59	68.34
1.5	160.83	132.19	96.37	78.01	72.66
2	173.42	137.67	113.76	90.78	82.01
24	185.31	141.09	120.28	95.03	87.05
48	220.97	171.91	131.15	100.70	93.52
96	223.77	184.93	141.30	112.05	97.84
120	225.87	187.67	145.65	117.77	101.43
144	227.97	190.41	147.82	119.85	105.03
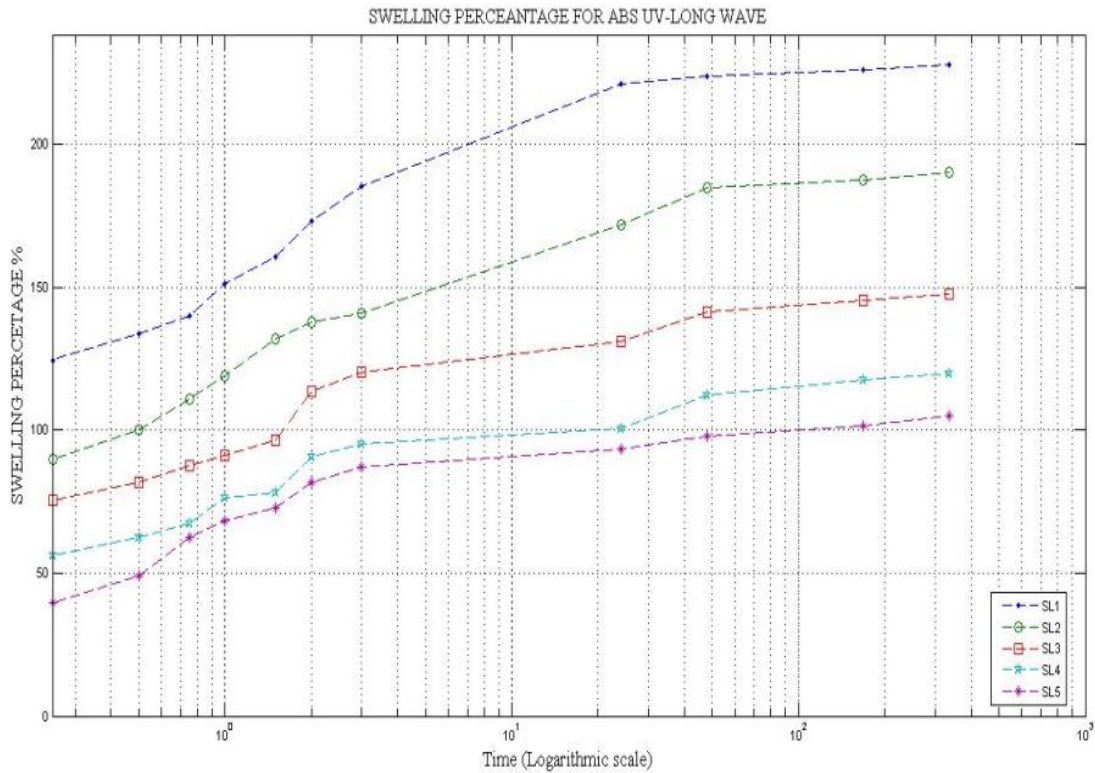
Figure 3.7: Swelling test ratios of SF biofilms UV-Long wave with ABS.

The swelling ratios were determined by equation (1) in chapter 2. As shown on Table 3.7 and Fig 3.7. For the acid buffer solution (pH = 1.2) samples prepared under long UV wave length, the pure SF biofilm increase in terms of swelling until it reached to its final swelling ratio value. It had the highest swelling ratio compared to the low crosslinked SF biofilm and the highly crosslinked SF biofilms. These indicate that as the crosslinker content increases in the biofilm the equilibrium swelling ratio decreases.

3.1.3 Swelling Test for Biofilms UV-Short wave 254nm With PBS

In this section, the swelling test applied to SF biofilms at phosphate buffer solution with pH = 7.404, which were prepared by UV-short wavelength and different amount of crosslinkers ($C_7H_{10}N_2O_2$) as shown on Table 3.8 and Figure 3.8

Figure 3.8: Swelling test for SF biofilms UV-short wave.

Table 3.8 Swelling values of SF biofilms UV-Short wave with PBS.

| Time(hours)	SS1(w)	SS2(w)	SS3(w)	SS4(w)	SS5(w)
0	12.2	12.3	11.8	12.4	12
0.25	46.2	45.7	36.3	27.1	25.1
0. 5	49.4	46.9	37.8	30.5	28.1
0.75	53.3	49.2	41.9	34.1	30.9
1	57.1	52.1	45.3	36.6	33.1
1.5	59.3	54.2	48.4	38.9	35.3
2	61.6	57.2	52.2	43.3	38.1
2.5	62.1	59.5	54.2	46.7	41.3
3.5	62.6	60.1	56.5	47.1	43.8
24	65.2	61.2	57.6	47.5	45.5
48	65.5	63.3	58.5	49.5	46.9
96	65.9	63.8	58.9	50	47.4
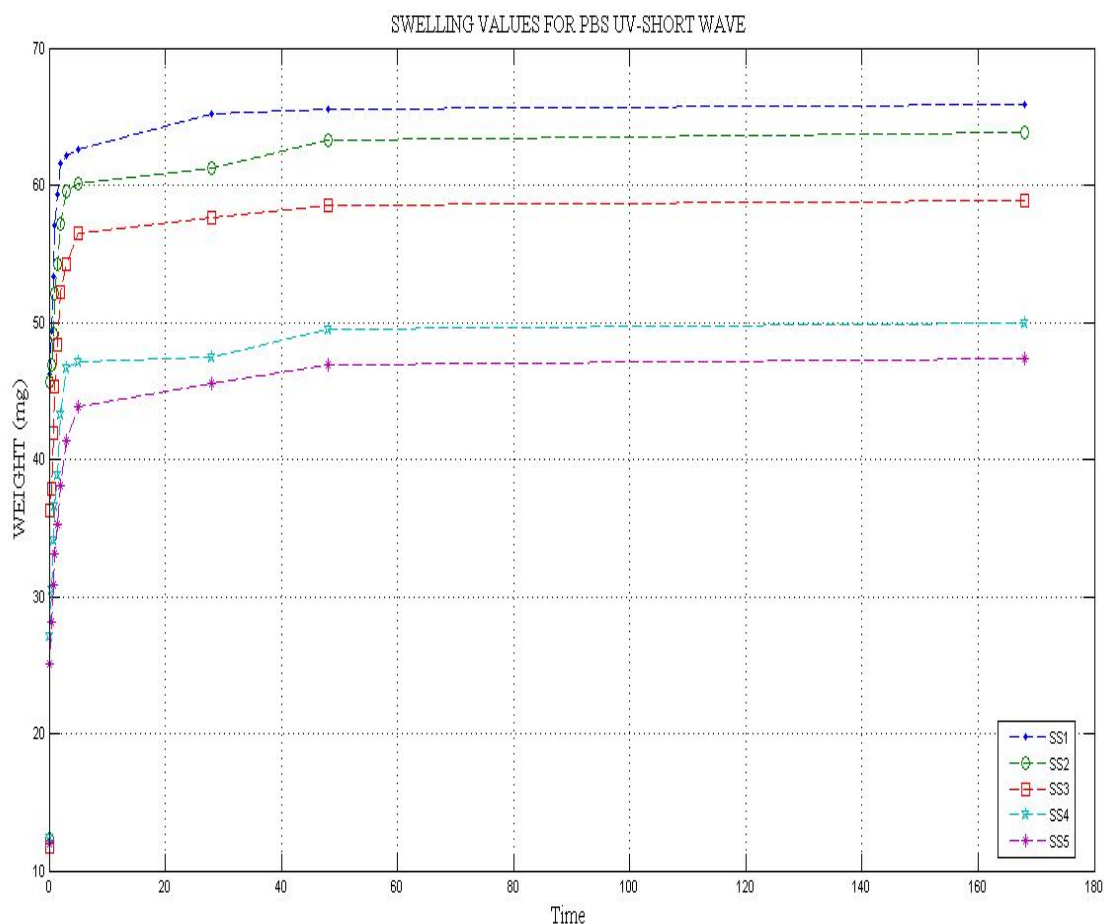
Figure 3.9: Swelling test values of SF biofilms UV-Short wave with PBS.

Same swelling test procedure was applied to the samples which were prepared by UV - Short wavelength (254 nm) and the results were shown on Table 3.8 and Figure 3.9. The biofilms prepared at short wavelength, the swelling ratios value was inversely proportional to the amount of crosslinker. By comparing with the biofilms prepared by long UV wavelengths they had a slower swelling ratio and their final swelling ratios surpass all the other biofilms prepared at long wavelength. This was related with the crosslink ratio of the UV-photopolymerization reaction. As the crosslink ratio increases biofilms becomes messier and pore sizes were decreased.

Table 3.9: Standard deviation for SF biofilms UV-Short wave with PBS.

| Samples	Total Numbers	Mean	Standard deviation	Variance(Standard deviation)	Population Standard deviation	Variance(Population Standard deviation)
SS1	12	55.03333	14.92785	222.84061	14.29233	204.27056
SS2	12	52.125	13.99598	195.8875	13.40013	179.56354
SS3	12	46.61667	13.56002	183.87424	12.98273	168.55139
SS4	12	38.75833	11.40235	130.01356	10.91692	119.1791
SS5	12	35.625	10.54343	111.16386	10.09456	101.90021
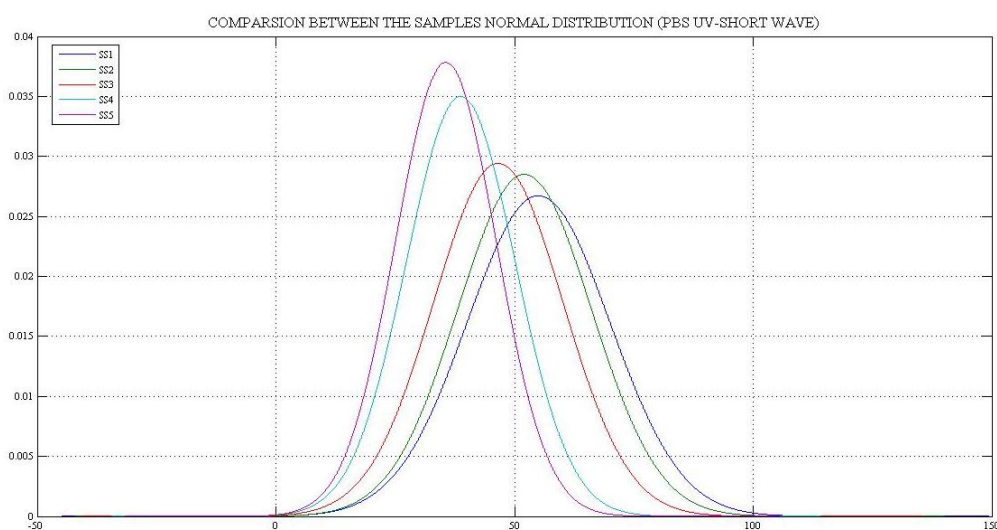
Figure 3.10: Normal distribution Biofilms UV-Short waves with PBS.

From table 3.9 and Fig. 3.10 showed the effect of crosslinker on the standard deviation and mean is inversely proportional with crosslinker amounts. The standard deviation value of the sample which prepared without crosslinker is 14.29, while, the standard deviation value of the sample which prepared with the highest crosslinker value 10.09.

Table 3.10: Swelling ratios of the SF biofilms UV-Short wave with PBS.

| Time(hours)	SS1(w)	SS2(w)	SS3(w)	SS4(w)	SS5(w)
0	0	0	0	0	0
0.25	278.68	271.54	207.62	118.54	109.16
0. 5	304.91	281.30	220.33	145.53	134.16
0.75	336.88	300	255.08	175.37	157.5
1	368.03	323.57	283.89	195.16	175.83
1.5	386.06	340.65	310.16	213.70	194.16
2	404.91	365.04	342.37	249.19	217.5
2.5	409.01	383.73	359.32	276.61	244.16
3.5	413.11	388.61	378.81	279.83	265.14
24	434.42	397.56	388.13	283.06	279.16
48	436.88	414.32	395.76	299.19	290.83
96	440	418.93	399.15	303.22	295.65
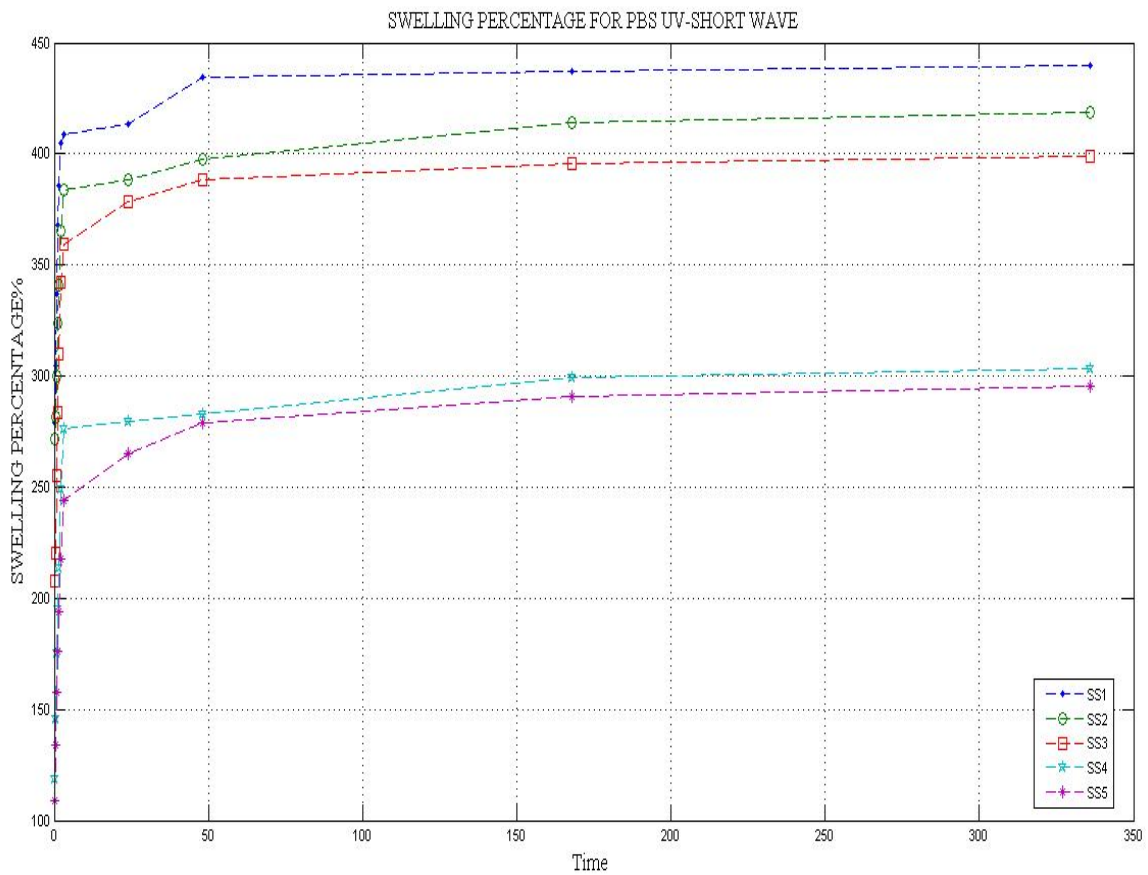
Figure 3.11: Swelling ratios of SF biofilms UV-Short wave with PBS.

This test also demonstrate the effect of crosslinker on the swelling process as well as comparing the difference between the samples which prepared in different conditions. The results which showed in Table 3.10 and Figure 3.11 indicated that the samples prepared under UV- Short wave generally swelled more than the samples which were prepared under UV-Long wave.

3.1.4 Swelling Test for Biofilms UV-Long wave Length 365nm with PBS

Table 3.11: Swelling test values of SF biofilms UV-Long wave with PBS.

Time(Hours)	SL1	SL2	SL3	SL4	SL5
0	14.1	14.5	13.9	14	14.2
0.25	48.8	46.4	37.5	31.8	30
0. 5	49.5	47.6	39	33.1	32.7
0.75	53.1	48.9	40.1	34	33.3
1	54.9	51.1	42.8	35.3	34.2
1.5	56.6	53.9	45.1	36.8	35.2
2	58.4	54.7	46.8	37.3	35.9
2.5	61.1	56	47.3	38	36.6
3.5	62.8	57.2	48.1	38.7	37.4
24	64	59.1	49.2	39.4	37.9
48	65.1	60.3	49.9	40.1	38.4
96	65.7	60.9	50.3	40.6	39
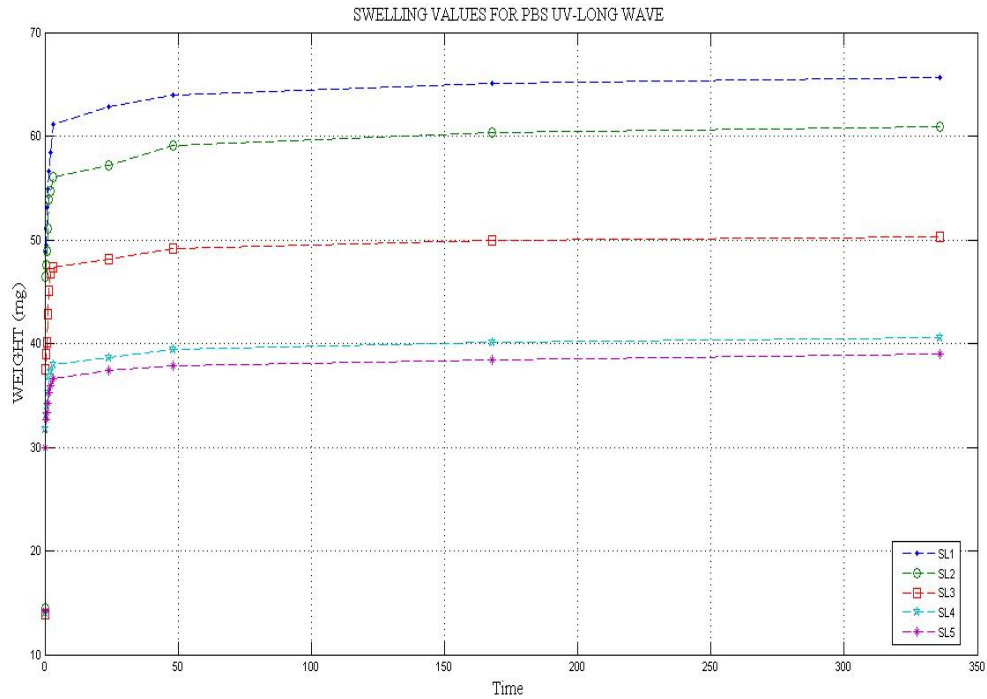
Figure 3.12: Swelling test for SF biofilms UV-Long wave with PBS.

Table 3.12: Swelling standard deviation for SF biofilms UV-Long wave with PBS.

| Samples	Total Numbers	Mean	Standard deviation	Variance(Standard deviation)	Population Standard deviation	Variance(Population Standard deviation)
SL1	12	54.50833	13.98665	195.62629	13.39119	179.3241
SL2	12	50.88333	12.44945	154.98879	11.91944	142.07306
SL3	12	42.5	10.00545	100.10909	9.57949	91.76667
SL4	12	34.925	7.15937	51.25659	6.85458	46.98521
SL5	12	33.73333	6.6902	44.75879	6.40538	41.02889
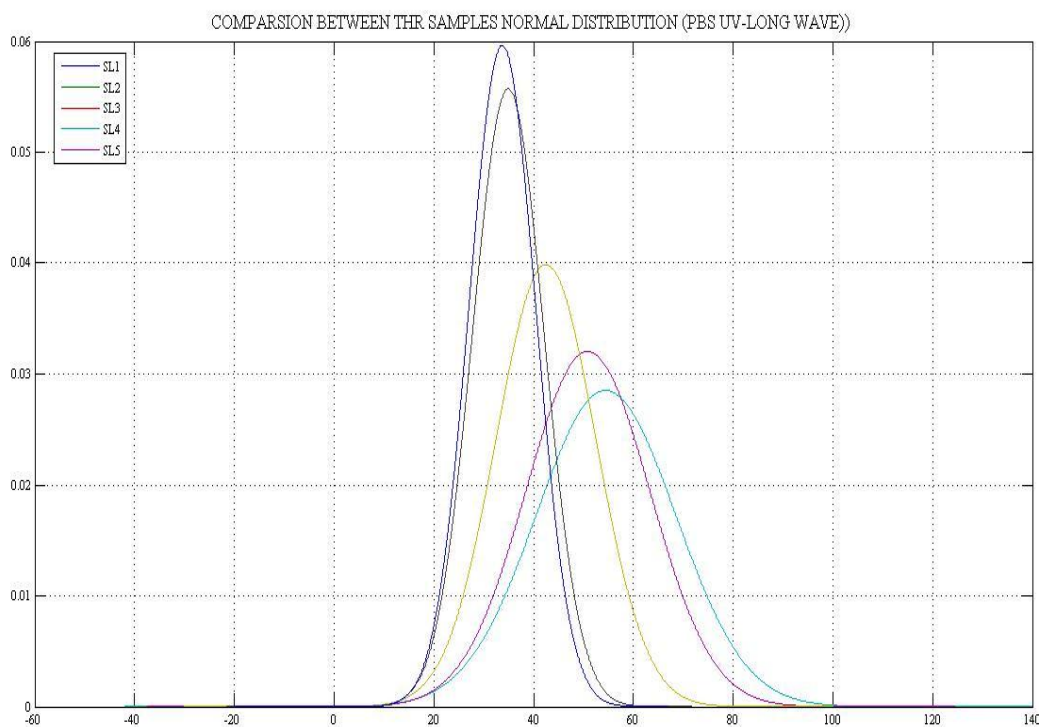
Figure 3.13: Normal distribution for Biofilms UV-Long waves with PBS.

According to the results of the standard deviation of silk fibroin biofilms, UV-Short wave with PBS swelling as showed in Table 3.12 and Fig 3.13, the sample SS5 has the lowest standard deviation value and mean. SS5 was prepared with 150 µl of $C_7H_{10}N_2O_2$ crosslinker. The sample SS1which was prepared without crosslinker has the highest standard deviation value and mean.

Table 3.13: Swelling ratios of the SF biofilms UV-Long wave with PBS.

Time(hours)	SL1	SL2	SL3	SL4	SL5
0	0	0	0	0	0
0.25	246.09	220	169.78	127.14	111.26
0. 5	251.06	228.27	180.57	136.42	130.28
0.75	276.59	237.24	188.48	142.85	134.50
1	289.36	252.14	207.91	152.14	140.84
1.5	301.41	271.72	224.46	162.85	147.88
2	314.18	277.24	236.69	166.42	152.81
2.5	333.33	286.20	240.28	171.32	157.74
3.5	345.39	294.48	246.04	176.42	163.38
24	353.90	307.58	253.95	181.73	166.90
48	361.70	315.86	258.99	186.25	170.42
96	365.95	320	261.87	190	174.64
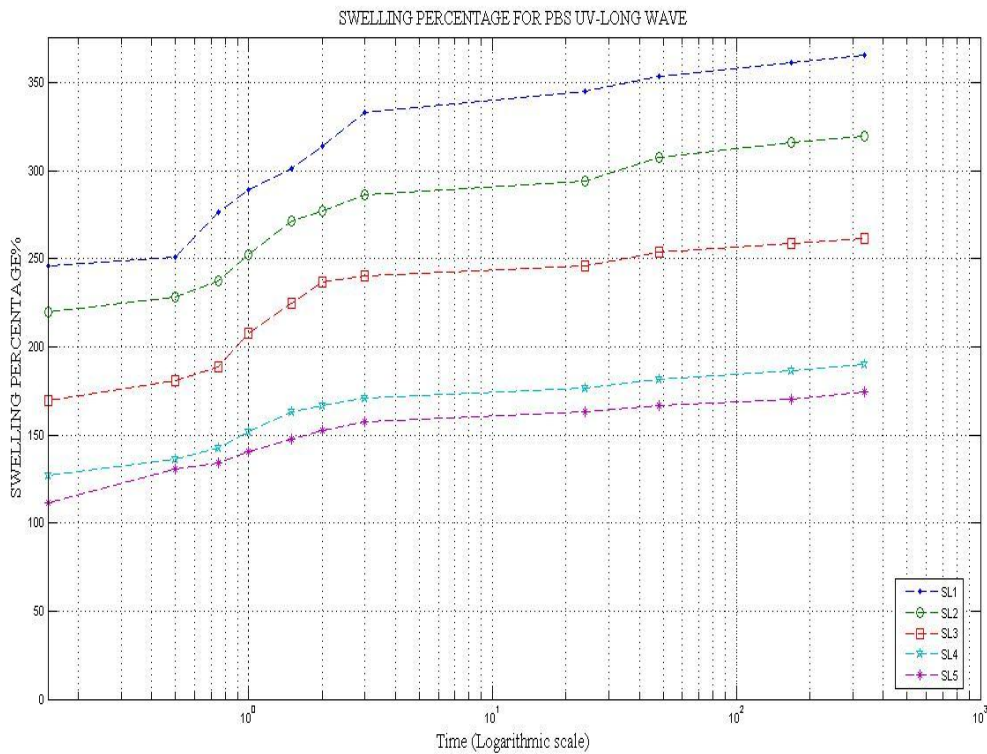
Figure 3.14: Swelling test ratios of SF biofilms UV-Long wave with PBS.

According to the results that showed in Table 3.13 and Fig 3.14 the effect of crosslinker was very clear. As the crosslinker amount increased the swelling ratio of the silk fibroin biofilm decreased.

As a result, swelling process showed high pH sensitivity. The SF / N, N' methylene diacrylamide biofilms may be useful as covering membranes in implantation process or carriers in drug delivery system. The crosslinked silk fibroin biofilms were insoluble in water and acid.

3.2 Biodegradation test

The silk fibroin biofilms biodegradation test was done by using protease enzyme weight per volume ratio 0.3 g/ml. The biofilms were tested within the enzyme solution at 37°C as showed in Figure 3.15.
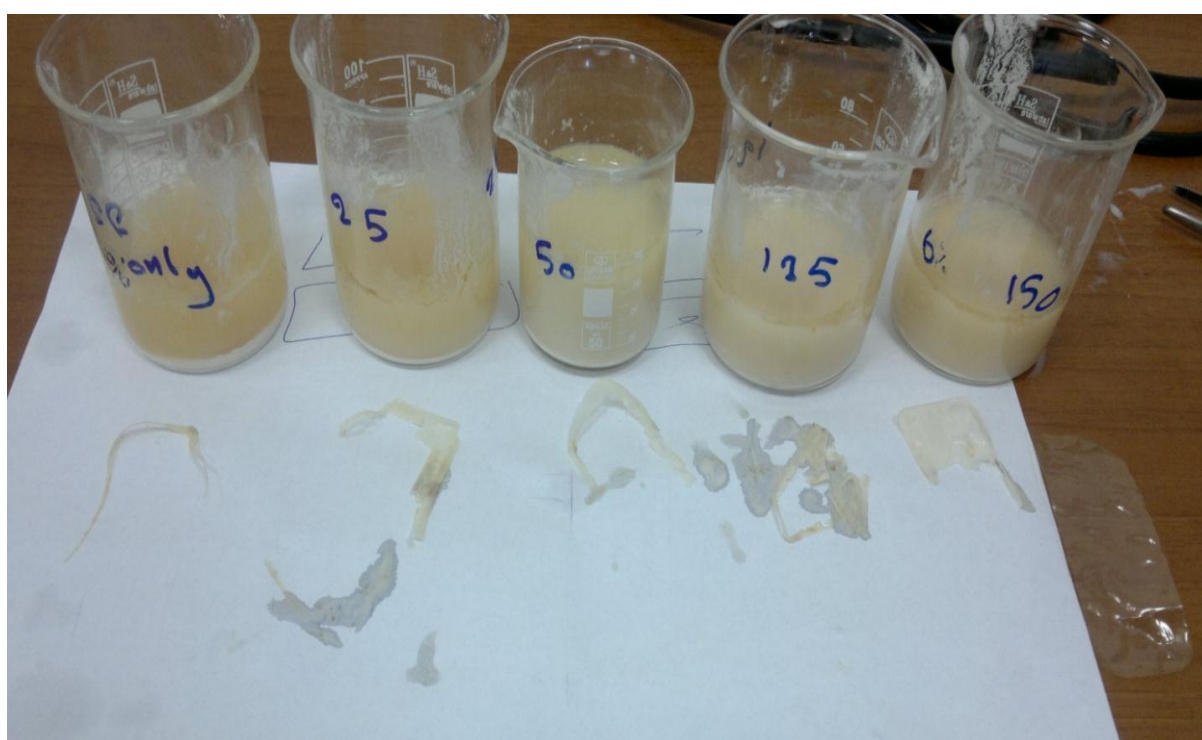
Figure 3.15: Biodegradation test for SF biofilms with protease enzyme.

3.2.1 Biodegradation test for biofilms UV-Short wave length with protease enzyme

Table 3.14: Biodegradation test for SF biofilms UV-Short wave with protease enzyme.

| Time(Hours)	SS1(w)	SS2(w)	SS3(w)	SS4(w)	SS5(w)
0	60.12	60.43	59.97	59.69	60
0.25	55.23	56.74	57.61	58.98	59.54
0.5	52.64	54.59	55.99	57.84	58.89
0.75	49.69	52.71	54.79	56.81	57.84
1	47.19	50.21	52.91	55.5	56.10
1.5	44.11	48.32	51	54.93	55.76
2	38.65	43.95	48.42	52.32	53.00
2.3	34.23	38.12	45.39	48.15	50.90
3	31.38	36.69	43.00	46.12	48.01
5	22.13	29.31	38.64	40.93	42.99
20	16.98	21.10	29.99	35.19	38.12
21	5.19	9.18	17.16	25.09	28.37
23	0	0	9.23	17.91	20.14
26	0	0	0	9.36	15.77
30	0	0	0	0	6.01
48	0	0	0	0	0
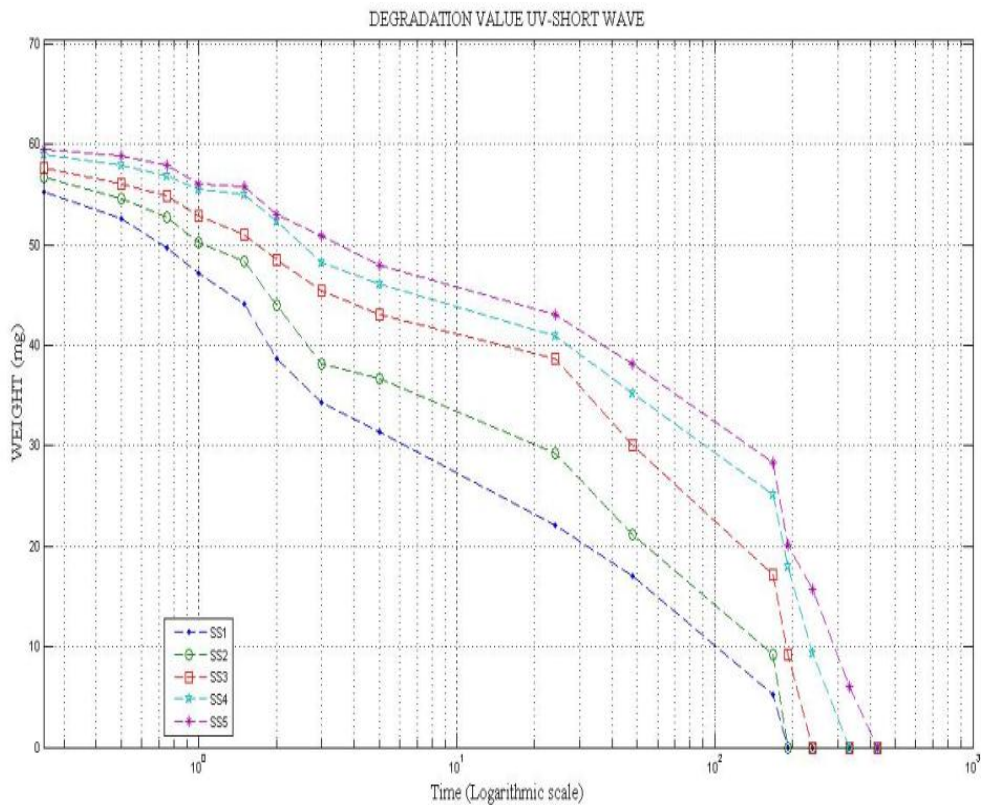
Figure 3.16: Biodegradation test for silk fibroin biofilms UV-Short wave length.

The biodegradation test results for biofilms prepared by UV-Short wave length were shown on Table 3.14 and Figure 3.16. The results indicated that, as the crosslinker amount increased in the preparation of biofilms the biodegradation rate was decreased. The samples which prepared by lowest amount of crosslinker (SS1, SS2, SS3) completely biodegraded within 26 hours, while the samples that were prepared with highest amount of crosslinker (SS4, SS5) did not biodegraded in 24 hours. All samples were completely biodegraded within 48 hours.

Table 3.15: Biodegradation Standard deviation for SF biofilms UV-Short wave.

Samples	Total Numbers	Mean	Standard deviation	Variance(Standard deviation)	Population Standard deviation	Variance(Population Standard deviation)
SS1	16	28.59625	22.28408	496.58041	21.57647	465.54414
SS2	16	31.33438	22.94262	526.36359	22.21409	493.46586
SS3	16	35.25625	22.49505	506.02742	21.78074	474.40071
SS4	16	38.67625	21.46725	460.84281	20.78558	432.04014
SS5	16	40.715	20.31888	412.85676	19.67367	387.05321
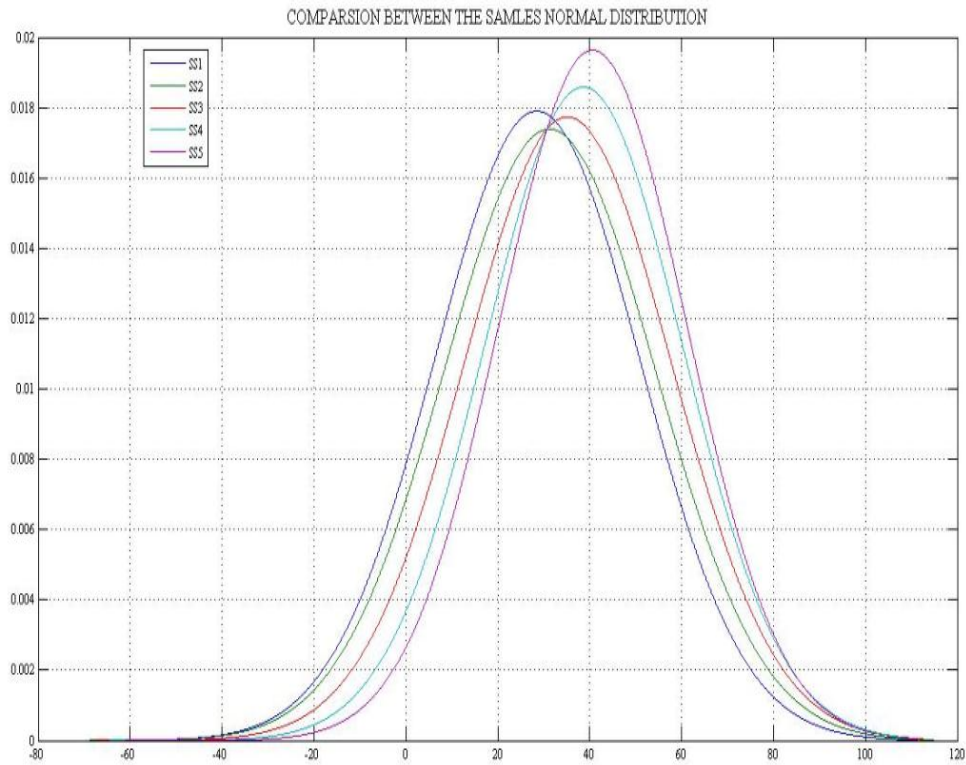
Figure 3.17: Biodegradation test standard deviation for SF biofilms UV-Short wave.

Table 3.16: Biodegradation test ratios for SF biofilms UV-Short wave.

| Time	SS1	SS2	SS3	SS4	SS5
0	100	100	100	100	100
0.25	91.86	93.89	96.06	98.81	99.23
0.5	87.55	90.33	93.36	96.81	98.15
0.75	82.65	87.22	91.36	95.17	96.47
1	78.49	83.08	88.22	93.06	93.52
1.5	73.36	79.96	85.04	92.02	92.93
2	64.28	72.72	80.74	87.65	88.33
2.3	56.93	63.08	75.68	80.66	84.83
3	52.19	60.71	71.70	77.26	80.01
5	36.80	48.50	64.42	86.57	71.65
20	28.24	34.91	50.00	58.95	63.53
21	8.63	15.19	28.61	42.03	47.28
23	0	0	15.39	30.00	33.56
26	0	0	0	15.68	26.28
30	0	0	0	0	10.01
48	0	0	0	0	0
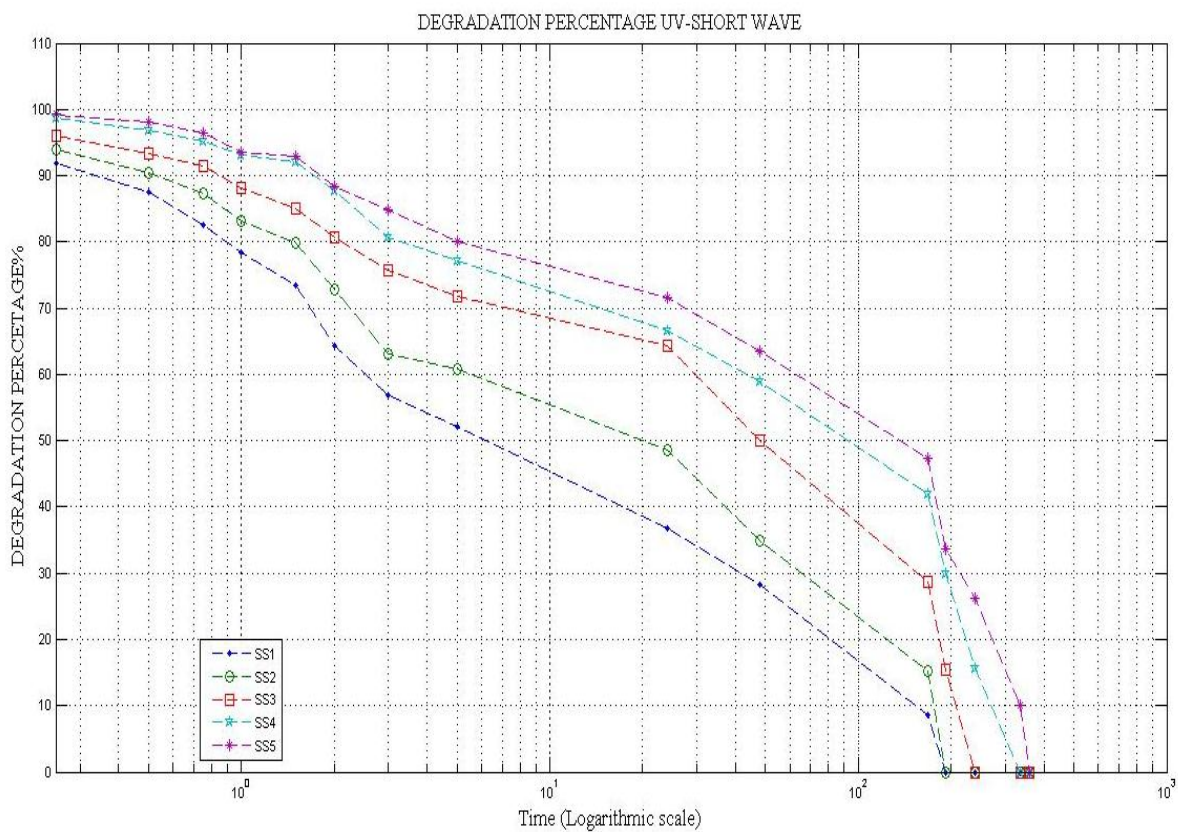
Figure 3.18: Biodegradation test ratios for SF biofilms UV-Short wave.

The degradation test results for biofilms prepared by UV-Short wave length were shown on Table 3.16 and figure 3.18. The results indicated that, as the crosslinker amount increased in the preparation of biofilms the biodegradation rate was decreased.

3.2.2 Biodegradation test for biofilms UV-Long wave with protease enzyme

Table 3.17: Biodegradation test values for SF biofilms UV-Long wave.

Time (Hours)	SL1	SL2	SL3	SL4	SL5
0	61.5	61.9	61.7	61.6	61
0.25	55.6	56.1	58.2	58.4	59.1
0.5	50.92	53.23	55.9	56.8	57.9
0.75	43.41	45.84	48.11	51.45	53.64
1	36	39.12	42.9	47.31	50.12
1.5	29.59	35.87	37.00	43.85	48.59
2	25.89	30.10	31.85	38.43	45.00
2.5	16.36	22.44	25.05	30.35	38.69
4	9.32	11.01	14.33	21.00	30.98
24	00.00	00	0	10.4	18.90
27	0	0	0	0	10.18
48	0	0	0	0	0
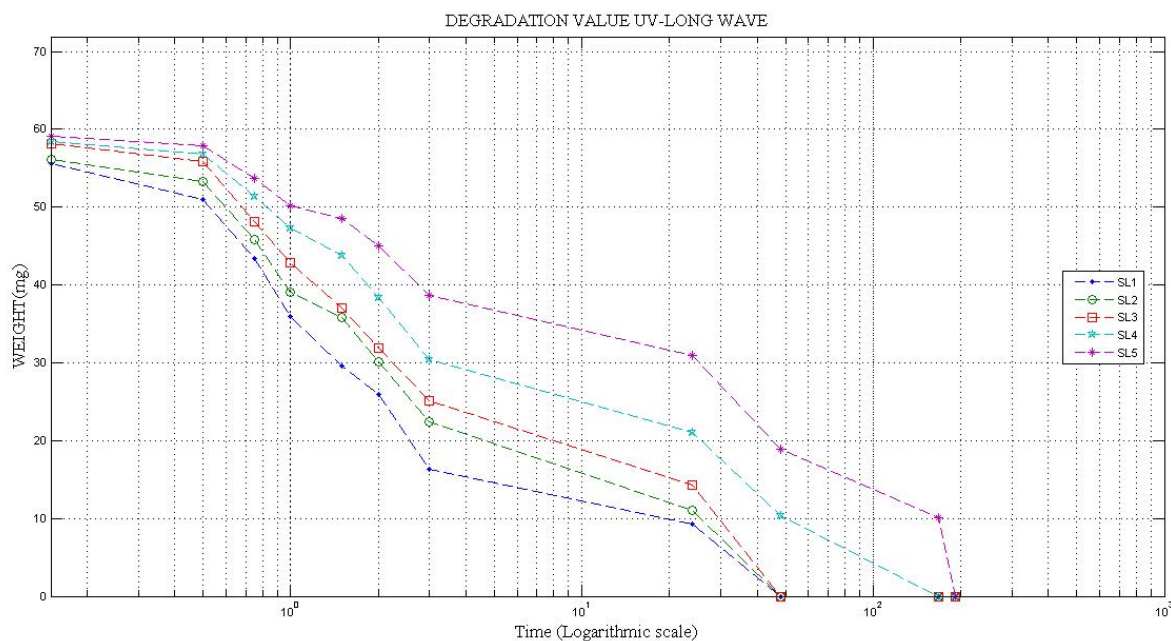
Figure 3.19: Biodegradation test values for SF biofilms UV-Long wave length.

The biodegradation test results for biofilms prepared by UV-Long wave length were shown on Table 3.17 and Figure 3.19. The results indicated that, as the crosslinker amount increased

in the preparation of biofilms the biodegradation rate was decreased. The samples which prepared by lowest amount of crosslinker (SL1, SL2, SL3) completely biodegraded within 24 hours, while the samples that were prepared with highest amount of crosslinker (SL4, S5) did not biodegraded in 24 hours. All samples were completely biodegraded within 48 hours.

Table 3.18: Biodegradation Standard deviation for SF biofilms UV-Long wave length.

Samples	Total Numbers	Mean	Standard deviation	Variance(Standard deviation)	Population Standard deviation	Variance(Population Standard deviation)
SL1	12	27.3825	22.46136	504.51282	21.50512	462.47009
SL2	12	29.63417	22.80982	520.28795	21.83874	476.93062
SL3	12	31.25333	23.29445	542.63144	22.30274	497.41216
SL4	12	34.96583	22.39187	501.39586	21.43858	459.61287
SL5	12	39.52667	20.26019	410.47546	19.39766	376.26917
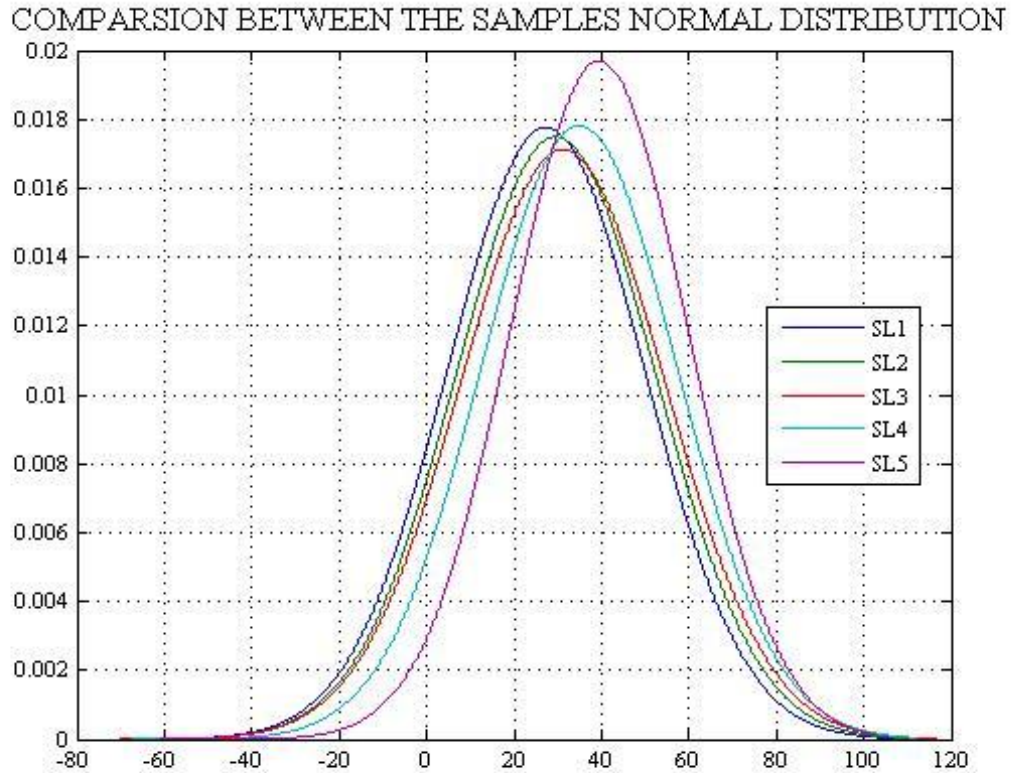
Figure 3.20: Biodegradation Standard deviations for SF biofilms UV-Long wave.

Table 3.19: Biodegradation test ratios for SF biofilms UV-Long wave.

Time	SL1	SL2	SL3	SL4	SL5
0	100	100	100	100	100
0.25	90.43	90.09	94.32	94.80	96.88
0.5	82.79	85.99	90.59	92.20	94.93
0.75	70.58	74.05	77.97	83.52	87.93
1	58.53	63.19	69.52	76.80	82.16
1.5	48.11	57.94	59.98	71.18	79.65
2	42.09	48.62	51.62	62.38	73.77
2.5	26.60	36.25	40.59	49.26	63.42
4	15.15	17.78	23.22	34.09	50.78
24	0	0	0	16.88	30.98
27	0	0	0	0	16.55
48	0	0	0	0	0
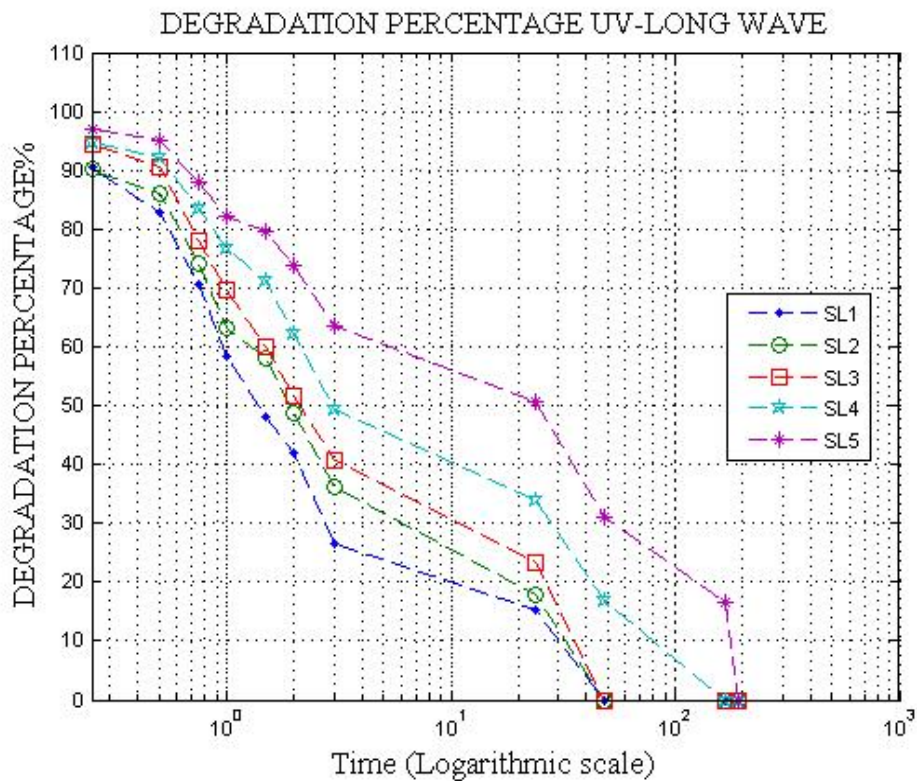
Figure 3.21: Biodegradation test ratios for SF biofilms UV-Long wave length.

The biodegradation ratio values were determined by using equation (2) in section 2. The results were shown in Table 3.19 and Figure 3.21 indicated that after half an hour from

the initial time, the biodegradation rate was increased for all samples without considering the crosslinker effect. After 24 hours, SL1(without crosslinker), SL2 and SL3 which have small amount of crosslinker were biodegraded completely while SL5 which had highest amount of crosslinker still keep about 30.98% from its own weight as shown in Table 3.19. In 48 hours, SL4 was also biodegraded, while SL5 still keep about 16.55% from its own weight. After 55 hours from the beginning the SL5 was also biodegraded completely. These results indicated that, the biodegradation rate can be easily controlled by the amount of crosslinker added to the reaction mixture. As the amount of crosslinker increases, it enhanced the formation of crosslinking sites and also β-sheet formation triggered. Structural control of the silk protein was also gained through physical crosslinks (β-sheets), resulting in roboust and stable thin material coating (Jiang et al, 2007).

3.3Scanning electron microscope (SEM) analyses
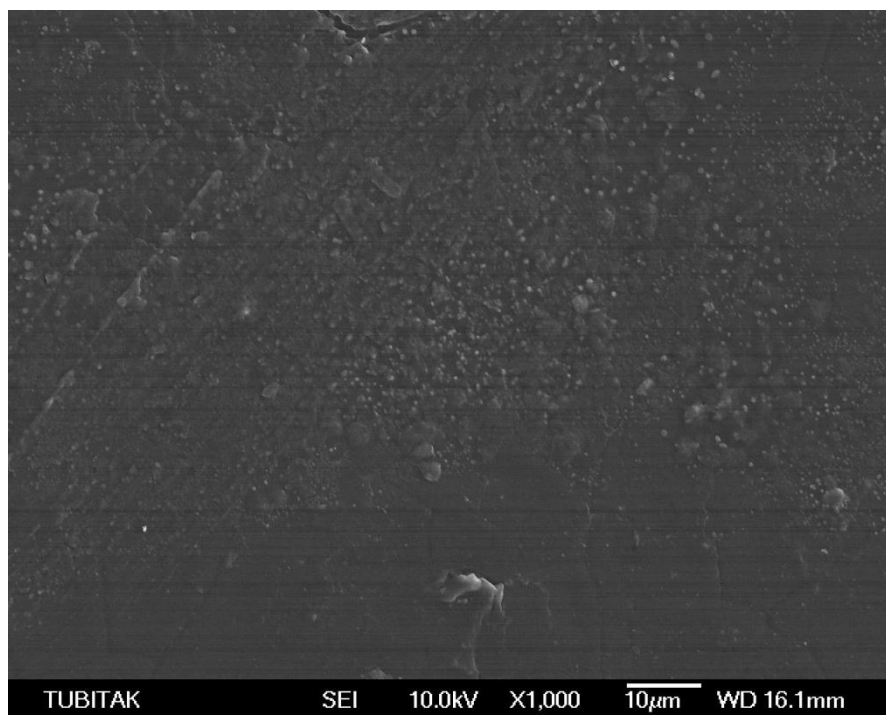
Figure 3.22: SEM analyses for SF biofilms without crosslinker.
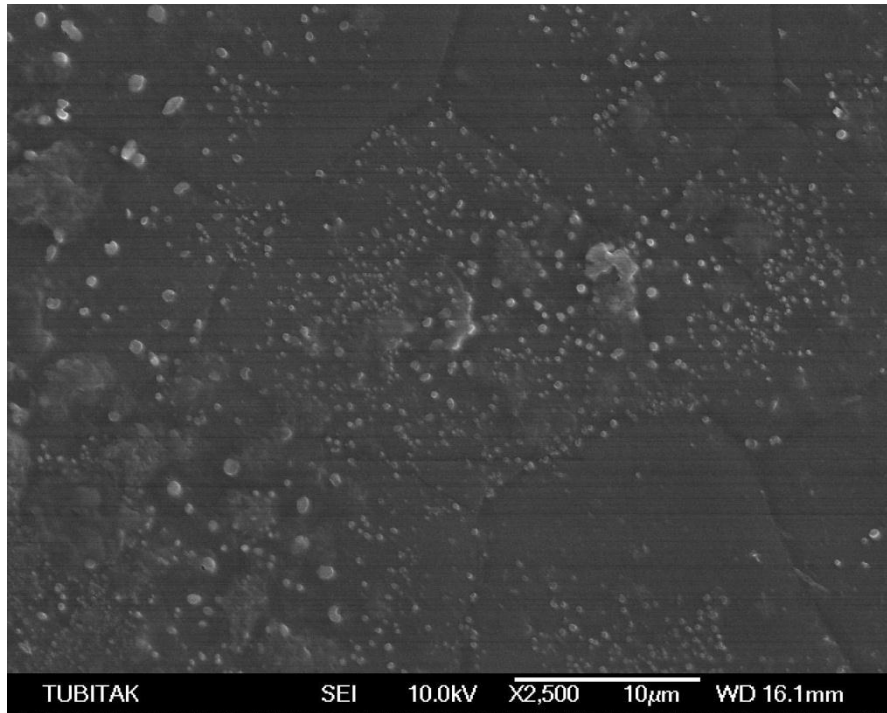
Figure 3.23: SEM analyses for SF biofilms with 25µl crosslinker.
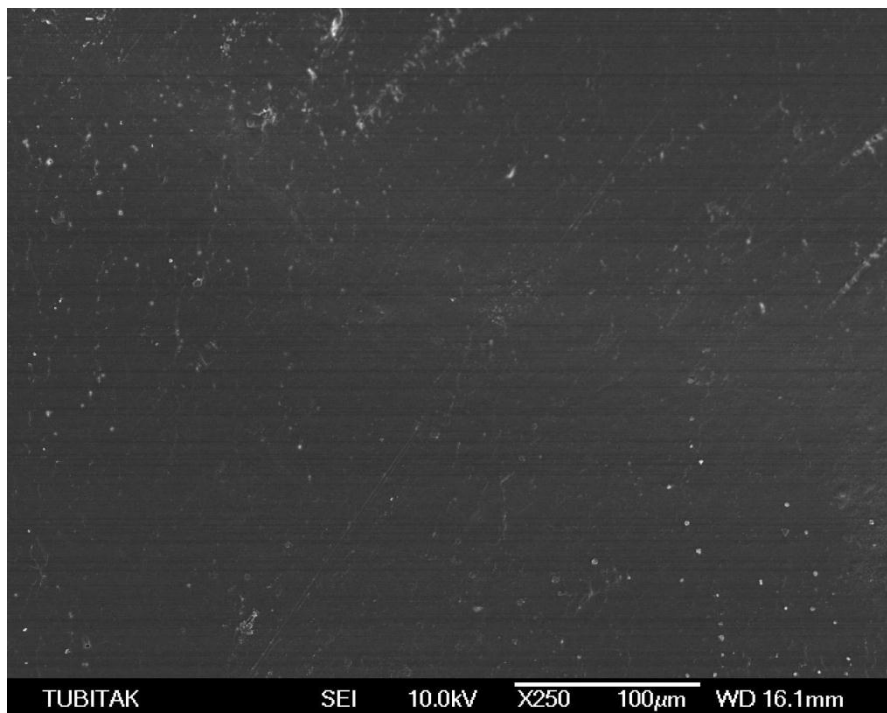
Figure 3.24 SEM analyses for SF biofilms with 50µl of crosslinker.
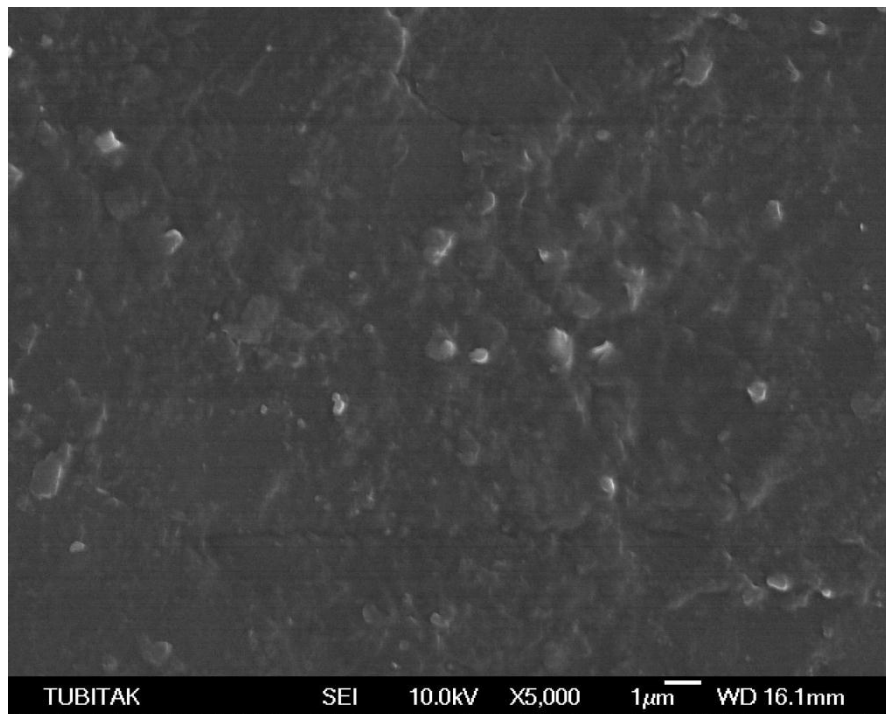
Figure 3.25: SEM analyses for SF biofilms with 125µl of crosslinker.
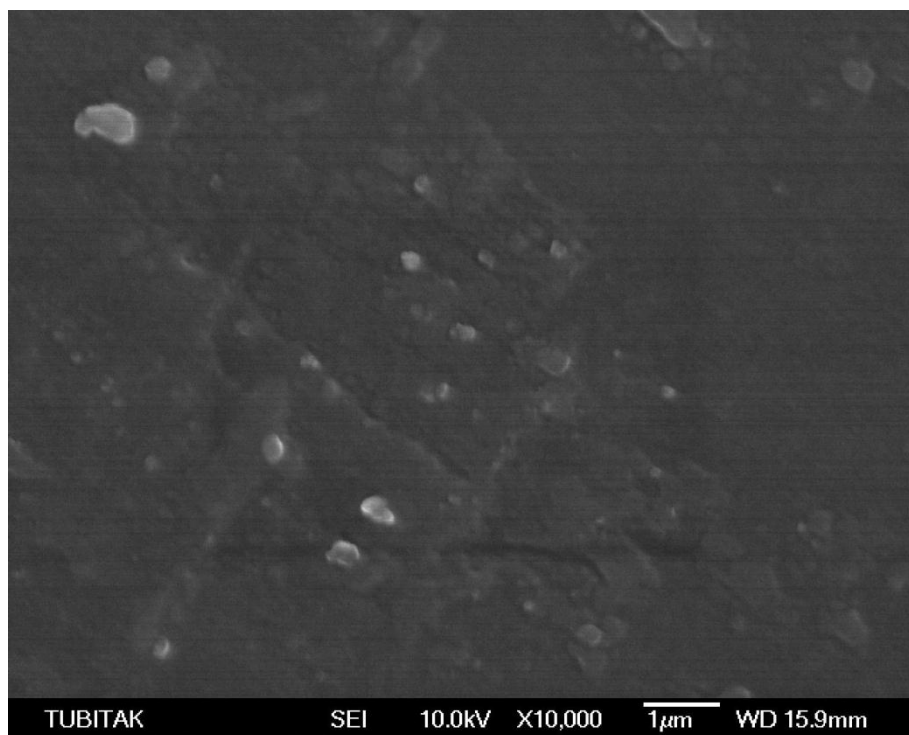

Figure 3.26: SEM analyses for SF biofilms with 150µl of crosslinker.

The SEM analyses showed that, the morphology of the silk fibroin biofilms have been changed as the amount of crosslinker ($C_7H_{10}N_2O_2$) varied within the preparation ratio. Different morphologies of the biofilms are attributed to the different modes of crosslinking,

and β-sheet formation. The highly crosslinked regions are separated from each other by well-defined thick fibroin network due to the highest amount of crosslinker during the preparation. Fig. 3.26 with 150 µl of crosslinker content showing SEM images of the thick fibroin biofilm formed at 254 nm wave length.

The SEM micrographs for silk fibroin biofilms also showed the crosslinker effects on the surface smoothness. The SEM micrographs for silk fibroin biofilms which prepared under UV –Short wave 254nm and UV-Long wave 365 nm indicate that the silk fibroin biofilms useful in cell culturing due to the porous structure and enable to cells proliferation and growth on the biofilm.

3.4 X-Ray Diffraction (XRD) Analyses

Table 3.20: X-Ray diffraction analyses of silk fibroin and silk fibroin biofilms prepared by UV-Short wave at 254nm.

samples	Strongest peak no.	2 theta (deg)	$d_{(A)}$	I/II	FWHM (deg)	Intensity (counts)	Integrated Int.(counts)
SFX(silk fibroin biofilms)	16	20.4200	4.345	100	0	111	0
	15	19.4800	4.553	86	0	95	0
	14	21.1800	4.191	86	0	95	0
Raw silk fibroin	6	11.620	7.609	100	2.240	37	3290
	11	20.560	4.316	76	2.100	28	2493
	5	10.46	8.4505	68	1.200	25	1099
SFS(silk fibroin scaffolds)	7	12.580	7.030	100	1.1600	17	1577
	15	20.500	4.328	100	1.400	17	1133
	4	4.120	9.688	94	1.040	16	1003

The X-Ray diffraction test results were summarized in Table 3.20. In the crosslinked samples weaker crystalline appeared at 12.58, 20.50, and 9.120. The raw silk fibroin samples gives three characteristic crystallinity peaks at 2 theta = 20.42, 19.48 and 21.180. The crystalline structure was affected as the amount of crosslinker increased in silk fibroin/ crosslinker ratio.
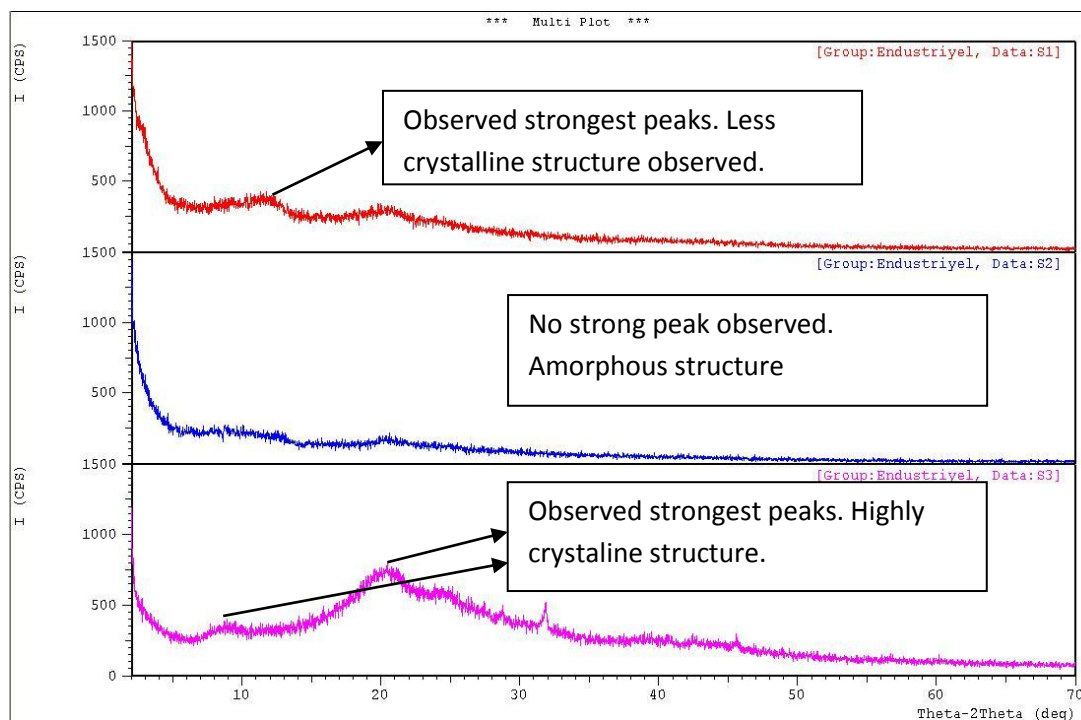
Figure 3.27: Comparison of (Data: S1) raw SF XDR pattern. (Data: S2) XDR pattern of SF scaffold prepared by freeze drying technique at 80C. (Data: S3) SF biofilms which prepared by UV induced photo polymerization technique under homogeneous conditions.

The XDR analysis for silk fibroin biofilms showed that the degree of crystallinity and the crystalline structure were affected by structural formation processes such as cross linker, the crosslinker help to formation ordered structure of silk fibroin biofilms.

3.5 *In-vitro* Coagulation Time Test Analyses

In this study, for the first time to our knowledge we analyzed the effect of crosslinker $C_7H_{10}N_2O_2$ on SF biofilms prepared by UV-irradiation under homogenous condition for determining plasma coagulation. Data were detected by measuring the activated partial thromboplastin time (APTT), prothrombin time (PTT), and INR by STA Compact Hemostasis System equipment, Stago, US. The results of *in-vitro* coagulation time tests were shown on the Table 3.21.

Table 3.21: The results of in-vitro coagulation time tests.

Sample	ActPT%	PTT	INR	APTT
Healthy Blood	114	0.93	12.7	25.9
SF Biofilm	113	0.93	12.9	26.1
Crosslinked SF Biofilm	110	1.01	13.4	26.3

The *in-vitro* coagulation time tests have been applied and results showed that the Prothrombin Time (PTT), APPT of the crosslinked SF biofilms prepared by casting method were higher than SF biofilms. This indicated that crosslinking ratio had an effect on the blood clotting period of time. As the β-sheet formation enhanced by adding crosslinker in the reaction mixture, the PTT and APPT were increased and improve the blood compatibility property of the biofilm. The biofilm exhibit high blood compatibility property making them good candidates as biomedical material for blood contacting devices.

**3.6 *In-vitro* Platelet Adhesion Analyses with Peripheric Seaming Method**
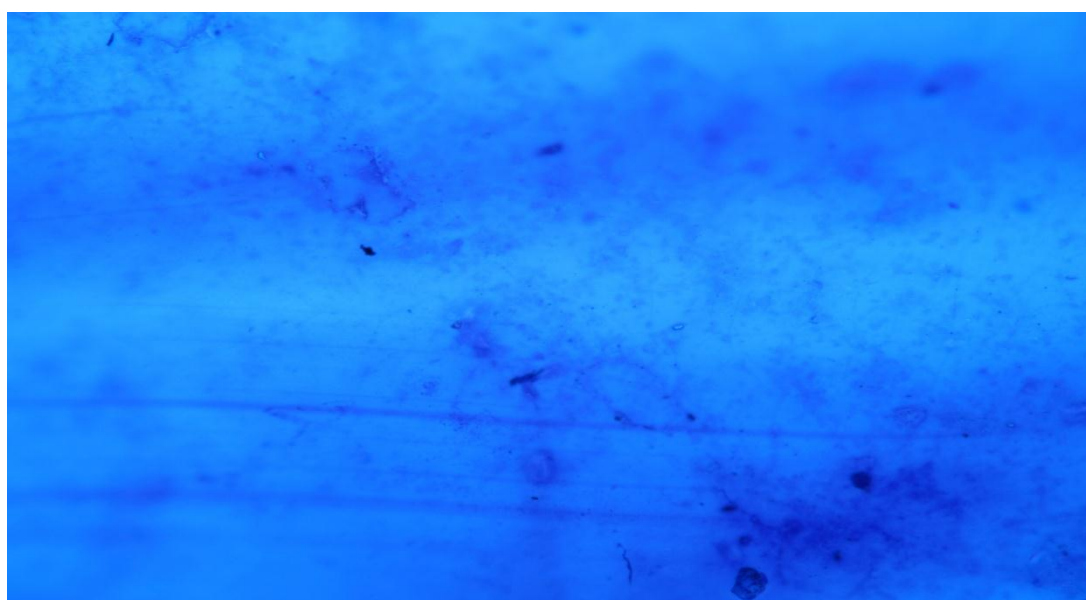
Figure 3.30: The electron microscope micrograph of SF crosslinked biofilm.

The *in vitro* peripheric seaming method was applied to analyzed platelet adhesion property of the prepared biofilms. The electron microscope micrograph of SF/ N, N'

methylene diacrylamide biofilms demonstrated that no platelet adhere on the surface of the biomaterial, as shown on Figure 3.30. The results indicated that the crosslinked SF biofilms could be considered as ideal candidates for biomedical applications.

Different forms of silk fibroin biofilms were prepared by UV induced photopolymerization technique under homogeneous conditions at short wave length 254 nm and long wave length 365 nm. The effects of crosslinker concentration, pH, and UV wave length were indicated on the physiochemical properties of the silk fibroin biofilms. Methanol treatment fixed the silk fibroin biofilms secondary structure. Due to the silk fibroin biofilms properties such as biocompatibility, biodegradability, and swelling gives the preference for silk fibroin biofilms to use it in the biomedical applications.

CHAPTER 4 CONCLUSIONS

Different forms of silk fibroin biofilms were prepared by UV induced photo polymerization technique under homogeneous conditions at short wave length 254 nm and long wave length 365 nm. The effects of crosslinker concentration, UV-wave length and different pH values were examined and their effects on the physiochemical properties of the silk fibroin biofilms have been shown. These films were characterized by SEM and XRD analysis and because of the formation of microstructure with crystalline β-sheets they improve their resistivity towards biodegradation and swelling properties can be controllable by the amount of crosslinker added to the reaction mixture. N, N' methyelene diacrylamide triggers the conformational transition of fibroin from random coil to β-sheet structure and hence fibroin film formation. One of the unique features is the blood compatibility property that allows to resists blood clotting and platelet adhesion.

These regenerated SF / N, N' methylene diacrylamide biofilms with their potential biocompatibility and physicochemical properties should provide value to a number of biomedical devices in the future.

References

Alessandrino, A., Marelli, B., Arosio, C., Fare, S., Tanzi, M. C., & Freddi, G. (2008). Electrospun silk fibroin mats for tissue engineering. *Engineering in life sciences*, 8(3), 219-225. http://onlinelibrary.wiley.com/doi/10.1002/elsc.200700067/abstract?deniedAccessCustomise dMessage=&userIsAuthenticated=false

Altman, G. H., Diaz, F., Jakuba, C., Calabro, T., Horan, R. L., Chen, J., ...& Kaplan, D. L. (2003). Silk-based biomaterials. *Biomaterials*, 24(3), 401-416.

Altman, G. H., Horan, R. L., Lu, H. H., Moreau, J., Martin, I, Richmond, J. C., & Kaplan, D. L. (2002). Silk matrix for tissue engineered anterior cruciate ligaments. *Biomaterials*, 23(20), 4131-4141. http://www.sciencedirect.com/science/article/pii/S0142961202001564

Altman, G. H., Horan, R. L., Lu, H. H., Moreau, J., Martin, I, Richmond, J. C., & Kaplan, D. L. (2002). Silk matrix for tissue engineered anterior cruciate ligaments. *Biomaterials*, 23(20), 4131-4141. http://www.sciencedirect.com/science/article/pii/S0142961202001564

Baimark, Y., Srihanam, P., Srisuwan, Y., & Phinyocheep, P. (2010). Preparation of porous silk fibroin microparticles by a water-in-oil emulsification-diffusion method. *Journal of Applied Polymer Science*, 118(2), 1127-1133. http://onlinelibrary.wiley.com/doi/10.1002/app.32506/abstract?deniedAccessCustomisedMes sage=&userIsAuthenticated=false

Benfenati, V., Pistone, A., Sagnella, A., Stahl, K., Camassa, L., Gomis-Perez, C., ... & Muccini, M. (2012). Silk fibroin films are a bio-active interface for neuroregenerative medicine. *Journal of applied biomaterials & functional materials*, 10(3), 315-323.

Bray, L. J., George, K. A., Ainscough, S. L., Hutmacher, D. W., Chirila, T. V., & Harkin, D. G. (2011). Human corneal epithelial equivalents constructed on< i> Bombyx mori</i> silk fibroin membranes. *Biomaterials*, 32(22), 5086-5091. http://www.sciencedirect.com/science/article/pii/S0142961211003668

Cao, Z., Chen, X., Yao, J., Huang, L., & Shao, Z. (2007). The preparation of regenerated silk fibroin microspheres. *Soft Matter*, 3(7), 910-915. http://pubs.rsc.org/en/content/articlelanding/2007/sm/b703139d#!divAbstract

Correia, C., Bhumiratana, S., Leping, Y., Oliveira, A. L., Gimble, J. M., Kaplan, D. L., ... & Reis, R. L. The Influence of Silk Fibroin 3D Scaffold Composition For *In Vitro* Bone Tissue Engineering. *Bone,* 70, 90.

Dobb, M. G., Fraser, R. D. B., & Macrae, T. P. (1967). The fine structure of silk fibroin. *The Journal of cell biology*, 32(2), 289-295. http://jcb.rupress.org/content/32/2/289.abstract

Enomoto, S., Sumi, M., Kajimoto, K., Nakazawa, Y., Takahashi, R., Takabayashi, C., ... & Sata, M. (2010). Long-term patency of small-diameter vascular graft made from fibroin, a silk-based biodegradable material. Journal of Vascular Surgery, 51(1), 155-164. http://dx.doi.org/10.1016/j.jvs.2009.09.005

Freddi, G., Anghileri, A., Sampaio, S., Buchert, J., Monti, P., & Taddei, P. (2006). Tyrosinase-catalyzed modification of *Bombyx mori* silk fibroin: Grafting of chitosan under heterogeneous reaction conditions. *Journal of biotechnology*, 125(2), 281-294. http://www.sciencedirect.com/science/article/pii/S0168165606001970

Freddi, G., Romanò, M., Massafra, M. R., & Tsukada, M. (1995). Silk fibroin/cellulose blend films: Preparation, structure, and physical properties. *Journal of applied polymer science*, 56(12), 1537-1545. http://onlinelibrary.wiley.com/doi/10.1002/app.1995.070561203/abstract

Freddi, G., Tsukada, M., & Beretta, S. (1999). Structure and physical properties of silk fibroin/polyacrylamide blend films. *Journal of applied polymer science*, 71(10), 1563-1571.

Gil, E. S., & Hudson, S. M. (2007). Effect of silk fibroin interpenetrating networks on swelling/deswelling kinetics and rheological properties of poly (N-isopropylacrylamide) hydrogels. *Biomacromolecules*, 8(1), 258-264. http://pubs.acs.org/doi/abs/10.1021/bm060543m

Gil, E. S., Frankowski, D. J., Spontak, R. J., & Hudson, S. M. (2005). Swelling behavior and morphological evolution of mixed gelatin/silk fibroin hydrogels. *Biomacromolecules*, 6(6), 3079-3087.http://pubs.acs.org/doi/abs/10.1021/bm050396c

Gotoh, Y., Tsukada, M., Baba, T., & Minoura, N. (1997). Physical properties and structure of poly (ethylene glycol)-silk fibroin conjugate films. *Polymer*, 38(2), 487-490. http://www.sciencedirect.com/science/article/pii/S0032386196006659

Gupta, V., Aseh, A., Ríos, C. N., Aggarwal, B. B., & Mathur, A. B. (2009). Fabrication and characterization of silk fibroin-derived curcumin nanoparticles for cancer therapy. *International journal of nanomedicine*, 4, 115. http://www.ncbi.nlm.nih.gov/pmc/articles/PMC2720745/

Hines, D. J., & Kaplan, D. L. (2011). Mechanisms of controlled release from silk fibroin films. *Biomacromolecules*, 12(3), 804-812.http://pubs.acs.org/doi/abs/10.1021/bm101421r

Hofmann, S., Wong Po Foo, C. T., Rossetti, F., Textor, M., Vunjak-Novakovic, G., Kaplan, D. L., ... & Meinel, L. (2006). Silk fibroin as an organic polymer for controlled drug delivery. *Journal of Controlled Release*, 111(1), 219-227. http://www.sciencedirect.com/science/article/pii/S0168365905007327

Hu, K., Lv, Q., Cui, F. Z., Feng, Q. L., Kong, X. D., Wang, H. L., ... & Li, T. (2006). Biocompatible fibroin blended films with recombinant human-like collagen for hepatic tissue engineering. *Journal of bioactive and compatible polymers*, 21(1), 23-37. http://jbc.sagepub.com/content/21/1/23.short

Hu, Y., Zhang, Q., You, R., Wang, L., & Li, M. (2012). The relationship between secondary structure and biodegradation behavior of silk fibroin scaffolds. *Advances in Materials Science and Engineering*. http://www.hindawi.com/journals/amse/2012/185905/

Imsombut, T., Srisuwan, Y., Srihanam, P., & Baimark, Y. (2010). Genipin-cross-linked silk fibroin microspheres prepared by the simple water-in-oil emulsion solvent diffusion method. *Powder Technology*, 203(3), 603-608. http://www.sciencedirect.com/science/article/pii/S0032591010003359

Jiang, C., Wang, X., Gunawidjaja, R., Lin, Y. H., Gupta, M. K., Kaplan, D. L., ...& Tsukruk, V. V. (2007). Mechanical properties of robust ultrathin silk fibroin films. *Advanced functional materials*, 17(13), 2229-2237. http://onlinelibrary.wiley.com/doi/10.1002/adfm.200601136/abstract

Jin, H. J., Chen, J., Karageorgiou, V., Altman, G. H., & Kaplan, D. L. (2004). Human bone marrow stromal cell responses on electrospun silk fibroin mats. *Biomaterials*, 25(6), 1039-1047. http://www.sciencedirect.com/science/article/pii/S0142961203006094.

Jin, H. J., Fridrikh, S. V., Rutledge, G. C., & Kaplan, D. L. (2002). Electrospinning Bombyx mori silk with poly (ethylene oxide). *Biomacromolecules*, 3(6), 1233-1239.http://pubs.acs.org/doi/abs/10.1021/bm025581u

Jin, H. Y., Yin, H., An, Y., Liu, Y., Wang, D. P., Liu, J., & Liu, X. (2012). Study on Biocompatibility of Post-Irradiated Silk Fibroin In Vitro. *Advanced Materials Research*, 535, 2357-2360. http://www.scientific.net/AMR.535-537.2357

Kasoju, N., & Bora, U. (2012). Silk Fibroin in Tissue Engineering. *Advanced healthcare materials*, 1(4), 393-412. http://onlinelibrary.wiley.com/doi/10.1002/adhm.201200097/full

Korte, W., Clarke, S., & Lefkowitz, J. B. (2000). Short activated partial thromboplastin times are related to increased thrombin generation and an increased risk for thromboembolism. *American journal of clinical pathology*, 113(1), 123-127. http://ajcp.ascpjournals.org/content/113/1/123.short

Kundu, J., Chung, Y. I., Kim, Y. H., Tae, G., & Kundu, S. C. (2010). Silk fibroin nanoparticles for cellular uptake and control release. *International journal of pharmaceutics*, 388(1), 242-250.

Kweon, H. Y., Woo, S. O., & Jo, Y. Y. (2010). Preparation and Characterization of Silk Fibroin Nanoparticles. *International Journal of Industrial Entomology*, 20(1), 25-28. http://www.papersearch.net/view/detail.asp?detail_key=0n601646

Kweon, H., Ha, H. C., Um, I. C., & Park, Y. H. (2001). Physical properties of silk fibroin/chitosan blend films. *Journal of applied polymer science*, 80(7), 928-934. http://onlinelibrary.wiley.com/doi/10.1002/app.1172/abstract?deniedAccessCustomisedMessage=&userIsAuthenticated=false

Lawrence, B. D., Marchant, J. K., Pindrus, M. A., Omenetto, F. G., & Kaplan, D. L. (2009). Silk film biomaterials for cornea tissue engineering. *Biomaterials,* 30(7), 1299-1308. http://www.sciencedirect.com/science/article/pii/S0142961208009095

Lawrence, B. D., Pan, Z., Weber, M. D., Kaplan, D. L., & Rosenblatt, M. I. (2012). Silk film culture system for in vitro analysis and biomaterial design. *Journal of visualized experiments: JoVE*, (62). http://www.ncbi.nlm.nih.gov/pmc/articles/PMC3466641/

Liu, H., Ge, Z., Wang, Y., Toh, S. L., Sutthikhum, V., & Goh, J. C. (2007). Modification of sericin-free silk fibers for ligament tissue engineering application. *Journal of Biomedical Materials Research Part B: Applied Biomaterials,* 82(1), 129-138. http://onlinelibrary.wiley.com/doi/10.1002/jbm.b.30714/full

Lu, Q., Wang, X., Hu, X., Cebe, P., Omenetto, F., & Kaplan, D. L. (2010). Stabilization and release of enzymes from silk films. *Macromolecular bioscience*, 10(4), 359-368. http://onlinelibrary.wiley.com/doi/10.1002/mabi.200900388/abstract?deniedAccessCustomis edMessage=&userIsAuthenticated=false

Luangbudnark, W., Viyoch, J., Laupattarakasem, W., Surakunprapha, P., & Laupattarakasem, P. (2012). Properties and biocompatibility of chitosan and silk fibroin blend films for application in skin tissue engineering. The Scientific World Journal, 2012. http://www.hindawi.com/journals/tswj/2012/697201/abs/

Ma, X., Cao, C., & Zhu, H. (2006). The biocompatibility of silk fibroin films containing sulfonated silk fibroin. *Journal of Biomedical Materials Research Part B: Applied Biomaterials*, 78(1), 89-96. http://onlinelibrary.wiley.com/doi/10.1002/jbm.b.30466/abstract?deniedAccessCustomisedM essage=&userIsAuthenticated=false

Mathur, A. B., & Gupta, V. (2010). Silk fibroin-derived nanoparticles for biomedical applications. *Nanomedicine*, 5(5), 807-820. http://www.futuremedicine.com/doi/abs/10.2217/nnm.10.51

Moraes, M. A. D., Nogueira, G. M., Weska, R. F., & Beppu, M. M. (2010). Preparation and characterization of insoluble silk fibroin/chitosan blend films. *Polymers*, 2(4), 719-727.http://www.mdpi.com/2073-4360/2/4/719

Motta, A., Maniglio, D., Migliaresi, C., Kim, H. J., Wan, X., Hu, X., & Kaplan, D. L. (2009). Silk fibroin processing and thrombogenic responses. *Journal of Biomaterials Science, Polymer Edition*, 20(13), 1875-1897.

Myung, S. J., Kim, H. S., Kim, Y., Chen, P., & Jin, H. J. (2008). Fluorescent silk fibroin nanoparticles prepared using a reverse microemulsion. *Macromolecular Research*, 16(7), 604-608. http://link.springer.com/article/10.1007/BF03218567#page-1

Nagarkar, S., Nicolai, T., Chassenieux, C., & Lele, A. (2010). Structure and gelation mechanism of silk hydrogels. *Physical Chemistry Chemical Physics*, *12*(15), 3834-3844. http://pubs.rsc.org/en/content/articlelanding/2010/cp/b916319k#!divAbstract.

Oh, S. H., & Lee, J. H. (2013). Hydrophilization of synthetic biodegradable polymer scaffolds for improved cell/tissue compatibility. *Biomedical Materials*, 8(1), 014101. http://iopscience.iop.org/1748-605X/8/1/014101

Patel, A. A., Thakar, R. G., Chown, M., Ayala, P., Desai, T. A., & Kumar, S. (2010). Biophysical mechanisms of single-cell interactions with microtopographical cues. *Biomedical microdevices*, 12(2), 287-296. http://link.springer.com/article/10.1007/s10544-009-9384-7#page-1

Pérez-Rigueiro, J., Elices, M., Llorca, J., & Viney, C. (2001). Tensile properties of silkworm silk obtained by forced silking. *Journal of Applied Polymer Science*, 82(8), 1928-1935. http://onlinelibrary.wiley.com/doi/10.1002/app.2038/full

Phillips, D. M., Drummy, L. F., Conrady, D. G., Fox, D. M., Naik, R. R., Stone, M. O., ...& Mantz, R. A. (2004). Dissolution and regeneration of Bombyx mori silk fibroin using ionic liquids. *Journal of the American chemical society*, 126(44), 14350-14351. http://pubs.acs.org/doi/abs/10.1021/ja046079f

Rajkhowa, R., Levin, B., Redmond, S. L., Li, L. H., Wang, L., Kanwar, J. R., ... & Wang, X. (2011). Structure and properties of biomedical films prepared from aqueous and acidic silk fibroin solutions. *Journal of Biomedical Materials Research Part A*, 97(1), 37-45. http://onlinelibrary.wiley.com/doi/10.1002/jbm.a.33021/abstract?deniedAccessCustomisedMessage=&userIsAuthenticated=false

Reddy, N., Jiang, Q., & Yang, Y. (2012). Biocompatible Natural Silk Fibers from Argema mittrei. *Journal of Biobased Materials and Bioenergy*, 6(5), 558-563. http://www.ingentaconnect.com/content/asp/jbmb/2012/00000006/00000005/art00006

S. Prasong, S. Wilaiwan and K. Nualchai. (2001).Structure and Thermal Characteristics of Bombyx mori Silk Fibroin Films: Effect of Different Organic Solvents", *International Journal of Chemical Technology 2(1):* 21-27, 2010 ISSN 1996-3416.

Sah, M. K., & Pramanik, K. (2010). Regenerated Silk Fibroin from B. mori Silk Cocoon for Tissue Engineering Applications. *Int. J. Environ. Sci. Technol*, 1, 404-408.

Sashina, E. S., Bochek, A. M., Novoselov, N. P., & Kirichenko, D. A. (2006). Structure and solubility of natural silk fibroin. *Russian journal of applied chemistry*, 79(6), 869-876. http://link.springer.com/article/10.1134/S1070427206060012#page-1

Sashina, E. S., Dubkova, O. I., Novoselov, N. P., Goralsky, J. J., Szynkowska, M. I., Lesniewska, E., ... & Strobin, G. (2009). Silver nanoparticles on fibers and films of Bombyx mori silk fibroin. *Russian Journal of Applied Chemistry*, 82(6), 974-980. http://link.springer.com/article/10.1134/S1070427209060081#page-1

Serban, M. A., Panilaitis, B., & Kaplan, D. L. (2011). Silk fibroin and polyethylene glycol-based biocompatible tissue adhesives. *Journal of Biomedical Materials Research Part A*,98(4),567-575. http://onlinelibrary.wiley.com/doi/10.1002/jbm.a.33149/abstract?deniedAccessCustomisedMessage=&userIsAuthenticated=false

Sukigara, S., Gandhi, M., Ayutsede, J., Micklus, M., & Ko, F. (2004). Regeneration of *Bombyx mori* silk by electrospinning. Part 2. Process optimization and empirical modeling using response surface methodology. *Polymer*, 45(11), 3701-3708. http://www.sciencedirect.com/science/article/pii/S0032386104003131

Sukigara, S., Gandhi, M., Ayutsede, J., Micklus, M., &Ko, F. (2003). Regeneration of *Bombyx mori* silk by electrospinning: Part 1: processing parameters and geometric properties. *Polymer*,44(19),5721-5727. http://www.sciencedirect.com/science/article/pii/S0032386103005329

Sun, M., Zhou, P., Pan, L. F., Liu, S., & Yang, H. X. (2009). Enhanced cell affinity of the silk fibroin-modified PHBHHx material. *Journal of Materials Science: Materials in Medicine*, 20(8), 1743-1751. http://link.springer.com/article/10.1007/s10856-009-3739-8#page-1

Teo, W. E., & Ramakrishna, S. (2006). A review on electrospinning design and nanofibre assemblies. *Nanotechnology*, 17(14), R89. http://iopscience.iop.org/0957-4484/17/14/R01

Thomson, R. C., Wake, M. C., Yaszemski, M. J., & Mikos, A. G. (1995). Biodegradable polymer scaffolds to regenerate organs. *In Biopolymers Ii (pp. 245-274). Springer Berlin Heidelberg.*

Uebersax, L., Mattotti, M., Papaloïzos, M., Merkle, H. P., Gander, B., & Meinel, L. (2007). Silk fibroin matrices for the controlled release of nerve growth factor (NGF). *Biomaterials*, 28(30), 4449-4460.

Valluzzi, R., Gido, S. P., Muller, W., & Kaplan, D. L. (1999*).* Orientation of silk III at the air-water interface. *International journal of biological macromolecules*, 24(2), 237-242. http://www.sciencedirect.com/science/article/pii/S0141813099000021

Vasconcelos, A., Gomes, A. C., & Cavaco-Paulo, A. (2012). Novel silk fibroin/elastin wound dressings. ActaBiomaterialia, 8(8), 3049-3060. http://www.sciencedirect.com/science/article/pii/S1742706112001821

Vepari, C., & Kaplan, D. L. (2007). Silk as a biomaterial. *Progress in polymer science*, 32(8), 991-1007.http://www.sciencedirect.com/science/article/pii/S0079670007000731

Wenk, E., Wandrey, A. J., Merkle, H. P., & Meinel, L. (2008). Silk fibroin spheres as a platform for controlled drug delivery. Journal of Controlled Release, 132(1), 26-34. http://www.sciencedirect.com/science/article/pii/S0168365908004628

Xu, Y., Wang, Y., Jiao, Y., Zhang, C., & Li, M. (2011). Enzymatic degradation properties of silk fibroin film. *Journal of Fiber Bioengineering and Informatics*, 4(1), 35-41.

Yamaura, K., Kuranuki, N., Suzuki, M., Tanigami, T., & Matsuzawa, S. (1990). Properties of mixtures of silk fibroin/syndiotactic-rich poly (vinyl alcohol). *Journal of applied polymer science*,41(9-10),2409-2425. http://onlinelibrary.wiley.com/doi/10.1002/app.1990.070410941/abstract

Yan, L. P., Oliveira, J. M., Oliveira, A. L., Caridade, S. G., Mano, J. F., & Reis, R. L. (2012). Macro/microporous silk fibroin scaffolds with potential for articular cartilage and meniscus tissue engineering applications. *ActaBiomaterialia*, 8(1), 289-301. http://www.sciencedirect.com/science/article/pii/S1742706111004302

Yang, Y., Ding, F., Wu, J., Hu, W., Liu, W., Liu, J., & Gu, X. (2007). Development and evaluation of silk fibroin-based nerve grafts used for peripheral nerve regeneration.

Biomaterials, 28(36), 5526-5535.
http://www.sciencedirect.com/science/article/pii/S0142961207007053

Yeo, J. H., Lee, K. G., Lee, Y. W., & Kim, S. Y. (2003). Simple preparation and characteristics of silk fibroin microsphere. *European Polymer Journal*, 39(6), 1195-1199. http://www.sciencedirect.com/science/article/pii/S0014305702003592

Zang, M., Zhang, Q., Davis, G., Huang, G., Jaffari, M., Ríos, C. N., ... & Mathur, A. B. (2011). Perichondrium directed cartilage formation in silk fibroin and chitosan blend scaffolds for tracheal transplantation. *ActaBiomaterialia*, 7(9), 3422-3431. http://www.sciencedirect.com/science/article/pii/S1742706111002054

Zarkoob, S. (1998). Structure and morphology of regenerated silk nano-fibers produced by electrospinning (Vol. 1, p. 77). http://adsabs.harvard.edu/abs/1998PhDT........77Z

Zarkoob, S., Reneker, D. H., Ertley, D., Eby, R. K., & Hudson, S. D. (2000). U.S. Patent No. 6,110,590. Washington, DC: U.S. Patent and Trademark Office. http://onlinelibrary.wiley.com/doi/10.1002/elsc.200700067/abstract?deniedAccessCustomise dMessage=&userIsAuthenticated=false

Zhang, Y. Q., Shen, W. D., Xiang, R. L., Zhuge, L. J., Gao, W. J., & Wang, W. B. (2007). Formation of silk fibroin nanoparticles in water-miscible organic solvent and their characterization. *Journal of Nanoparticle Research*, 9(5), 885-900. http://link.springer.com/article/10.1007/s11051-006-9162-x#page-1

Zhao, Z., Chen, A., Li, Y., Hu, J., Liu, X., Li, J., ...& Zheng, Z. (2012). Fabrication of silk fibroin nanoparticles for controlled drug delivery. *Journal of Nanoparticle Research*, 14(4), 1-10. http://link.springer.com/article/10.1007/s11051-012-0736-5#page-1

Zhou, P. (2011). Degradable PHBHHx Modified by the Silk Fibroin for the Applications of Cardiovascular Tissue Engineering. *ISRN Materials Science*, 2011. http://www.hindawi.com/isrn/materials.science/2011/389872/